Title
The evolution of the baculum in the extant and extinct Canidae

Author
Varajão de Latorre, Daniel

Publication Date
2022

Peer reviewed|Thesis/dissertation

The evolution of the baculum in the extant and extinct Canidae

by

Daniel Varajão de Latorre

A dissertation submitted in partial satisfaction of the

requirements for the degree of

Doctor of Philosophy

in

Integrative Biology

in the

Graduate Division

of the

University of California, Berkeley

Committee in charge:

Professor Charles R. Marshall, Chair
Professor Eileen Lacey
Professor Seth Finnegan
Professor Erica Bree Rosenblum

Summer 2022

The evolution of the baculum in the extant and extinct Canidae

Abstract

The evolution of the baculum in the extant and extinct Canidae

by

Daniel Varajão de Latorre

Doctor of Philosophy in Integrative Biology

University of California, Berkeley

Professor Charles R. Marshall, Chair

The genitalia of males evolves rapidly and divergently in most animal groups. Explanations for this pattern typically evoke mechanisms of post-copulatory sexual selection, such as sperm competition, cryptic female choice, and sexual conflict. While the fossil record often allows for the documentation of patterns of evolutionary change, the predominantly soft-tissue nature of the genitalia is rarely observed in the fossil record. However, the baculum (*os penis* or *os priapi*), a bone located at the distal end of the penis of most mammalian species, offers the opportunity of examining the evolution of male genitalia, and thus may contribute to our understanding of post-copulatory sexual selection and the evolution of reproductive biology within mammals. Bacula are rare in the fossil record and thus difficult to be identified and classified when in isolation. Nonetheless, sometimes they are preserved in association with other skeletal material allowing accurate species-level taxonomic assignments. Here, I focus on the bacula of the Canidae, which consists of three subfamilies, the extant Caninae (wolves, coyotes, jackals, foxes, etc.) and two extinct subfamilies, the Borophaginae and the Hesperocyoninae, both of which have rich fossil records that reveal high taxonomic and ecomorphological diversity.

This dissertation consists of four chapters. In the first chapter, I briefly contextualize the theory of post-copulatory sexual selection and then I review the evidence that it acts on the baculum from a combination of studies that used functional, experimental, and comparative data.

In Chapter 2 I describe the morphology of fossil bacula of five species of Borophaginae. These descriptions add substantial knowledge regarding the baculum of extinct canids, which was previously known for only two extinct species. The five bacula were found associated with other skeletal elements that were already described in the literature and have enabled identification to the species level. These borophagine bacula share many similarities with extant canines such as being robust, having a urethral groove, and a simple distal end. Because these features have been associated with reproductive strategies in extant carnivorans it is

possible to use the baculum of Borophaginae to draw implications for their reproductive biology.

In Chapter 3 I quantify variation in morphology of the baculum of canids in 2D using elliptic Fourier analysis. First, I show that the baculum of 26 (out of ∼35) extant species is morphologically conserved and that the intraspecific morphological variation is larger than the interspecific differences, and therefore it is difficult to distinguish among species using bacular morphology alone. However, four extinct canids that have completely preserved bacula show morphological differences from the extant canids. In particular, one morphological feature, the primary curvature of the baculum, differentiates the baculum of three stem group canids from those of extant species. I used phylogenetic ancestral state reconstruction to show that it would be unlikely to predict the arched curvature of the baculum observed in the stem fossils from the morphology observed in extant species.

Finally, in Chapter 4, I examine the relative size of the canid baculum. Using a linear regression corrected for phylogeny, I show a slightly negative allometric relationship between baculum length and body size in canids. Further, an isometric relationship cannot be rejected. These results are in contrast with the strong negative allometric relationships that have been described for other mammalian clades. Of particular interest are the relative size of fossil bacula. The baculum of *Hesperocyon gregarius*, the only known in the Hesperocyoninae, is significantly longer than expected for its body size and suggests a different allometric curve for this species in comparison with other canid groups. The bacula of two borophagine species are within the same allometric line of extant canids. Finally, the baculum of the extinct dire wolf (*Aenocyon dirus*) is longer than expected based on its body size, suggesting that its reproductive strategies could be different from those of extant canines.

To Débora Y. C. Brandt

Contents

List of Figures

List of Tables

Acknowledgments

It is incredible to get to this point of my Ph.D. and realize how many people have helped me along the way, some probably don't even know they helped me. Although the academic support is invaluable and has been crucial to getting here, there has been plenty of moments in which all I needed was companionship outside of academia and to connect with the rest of the world. I feel very thankful to all that have supported me in any way. I am also grateful for the remarkable number of opportunities offered to me just because I am a grad student in a place like Berkeley. These experiences widened my worldview and provided personal growth in a way I would never have imagined when I decided to embark on the PhD journey. I am bound to unjustly not include several people if I attempt a comprehensive list, but there are a few that I would like to thank nominally:

Words won't ever make justice to how grateful I am for having been advised by Charles Marshall! Thank you for the guidance, dedication, patience, support, advice, encouragement, and general care. Also, thank you for teaching science with inspiring enthusiasm, which I will always remember.

Eileen Lacey, thank you for the extensive feedback on all my chapters, which greatly improved my dissertation and increased my confidence in my work. I really appreciate your careful comments and edits.

Seth Finnegan and Bree Rosenblum for continuous encouragement since my second year, during quals, and the discussions that led me to the idea to study the baculum of mammals. Thank you also for the support when those ideas changed until they finally became this dissertation. I feel very lucky to have such a caring and positive dissertation committee.

Monica Albe, thanks for making the administrative hurdles easier.

How to ever explain the importance of my lab mates Camilla, Lucy, Jun, Kat, Josh, Ash, Connor, and Tanner? Thank you all for putting up with me daily, for excellent science discussions, for teaching me so much about the US, for guidance through life as a PhD student, and for being awesome friends!

Connor and Inessa, thank you for trusting me as a mentor in some of your first projects in science! And for making my job as a mentor so easy.

Cindy Looy, Ivo Duijnstee, and Seth Finnegan for organizing yearly UCMP field trips in which I learned so much!

Many other people made my time at Berkeley and the UCMP enjoyable and enriching, in particular Pat Holroyd, Lisa White, and Helina Chin.

Débora, I wouldn't have finished this PhD without you by my side. Thank you for being my home and love, for putting up with me through the worst, and for being the best moments of my life.

And finally, thank you to all my friends and family members that helped so much in keeping my mental health during the hardest times of PhD life, especially during a pandemic.

Chapter 1

General Introduction

The baculum, also called the penis bone, *os penis*, or *os priapi*, is located at the distal end of the penis. It is present in most species of placental mammals and shows high levels of interspecific morphological variation, a pattern common for structures associated with the transfer of gametes between individuals in the animal kingdom. During the last two decades, a growing number of studies have suggested that the morphological diversity of the baculum is at least partially explained by post-copulatory sexual selection. Here, I briefly summarize the concept of post-copulatory sexual selection and then review evidence that it acts on the baculum drawn from studies that use functional, experimental, and comparative data.

1.1 Post-copulatory sexual selection

Internal fertilization has evolved independently in multiple groups of animals and is present in the majority of the living animal species today. This reproductive strategy is often associated with the evolution of anatomical structures involved in the transfer of gametes, the intromittent genitalia, which are almost always present in males (Eberhard, 1985). The primary role of these structures is to transport gametes from males to females, although a few exceptions exist (*e.g.*, seahorses, Eberhard, 1985) in which females transfer the eggs to the males. The transfer of sperm is a straightforward function and can be achieved by organisms with simple genitalia. However, other mechanisms must be evoked to explain the remarkable variation in shape and size of intromittent organs that exists even among closely related species (Eberhard, 1985), which means that genitalia evolve quickly and divergently. Currently, the most widely favored explanation for the evolution of animal genitalia is based on mechanisms of post-copulatory sexual selection (Hosken & Stockley, 2004; Simmons, 2014; Brennan & Prum, 2015). Post-copulatory sexual selection is comprised of three non-mutually exclusive (and difficult to differentiate empirically) processes: sperm competition, female cryptic choice, and sexual conflict.

Sperm competition was first proposed by Parker (1970) as one of the selective forces that can bias the fertilization success of individual males. In particular, when a female

mates with two or more males during a single round of reproduction, sperm from the males may compete for fertilization of the ova and selection should favor male attributes that increase the probability of successful fertilization. Males have evolved multiple traits that are thought to reflect sperm competition, including sperm morphology and motility, the ability to deposit ejaculate in places that increase the chance of sperm reaching the ova, removal of ejaculate from previous males, and copulatory plugs that reduce the chances of insemination by subsequent mates. These strategies often involve morphological evolution of genital traits. For example, the tip of the penis of a damselfly (*Calopteryx maculata*) is flexible and extensible in a such way that it removes the sperm deposited in the female's spermatheca by previous males (Waage, 1979).

Cryptic female choice is the female oriented process of post-copulatory sexual selection, which is also postulated to be important in driving the evolution of male genitalia (Eberhard, 1985). Specifically, female traits that influence which male sperm fertilize eggs should lead to selection on males to either capitalize upon or avoid those determinants of fertilization success. In this context, copulation can be viewed as the last stage of courtship and subsequent female choice is considered "cryptic" because it occurs within the reproductive tracts of females and thus is not directly visible to researchers.

Finally, sexual conflict arises when the adaptive interests of males and females oppose each other, such that traits that are beneficial to males are costly to females and vice versa (Parker, 1979, and see Arnqvist & Rowe, 2005 for a review). Sexual conflict may happen at any stage of reproductive interactions between males and females; if it occurs during or after copulation it may affect the evolution of the genitalia. For example, males in many duck species engage in forced copulations with females, thereby generating a conflict over control for fertilization that is thought to have favored the evolution of complex vaginal structures that help to prevent forced insemination (Brennan *et al.*, 2007, 2010).

1.2 The baculum

In the late 1800s and early 1900s, descriptions of the baculum of different taxonomic groups revealed its morphological diversity. Multiple authors highlighted its usefulness for establishing evolutionary relationships among taxa (*e.g.*, Pocock, 1923; Chaine, 1926; Burt, 1936; White, 1953; Packard, 1960; Best & Schnell, 1974). For example, Pocock (1923) noted that the variability of the baculum of some rodents makes it useful for delineating relationships within but not among families. Burt (1960) used the baculum to infer the relative times of origin among groups after noticing that the bacula of mustelids are more diverse than those of canids, inferring that the canid species diverged more recently from each other than had the mustelids.

Despite this empirical work, hypotheses regarding the function of the baculum were scarce until the mid 1900s and to this day only a few papers have tried to identify the mechanisms responsible for driving the interspecific morphological differentiation of bacula. Long & Frank (1968) hypothesized that the baculum adds rigidity to the penis which may be

important for initiating intromission. Patterson & Thaeler (1982) argued that the evolution of bacula is not the result of neutral processes (Burt, 1936), or the result of pleiotropic effects acting on other parts of the organism (Mayr, 1963). Instead, they demonstrated that levels of intraspecific variability in the baculum is similar to other bones, that bacular structure has discrete distributions among different species, and that average bacular length correlates with average vaginal depth, all of which were considered evidence against the evolution of bacula via neutral processes. Further, Patterson & Thaeler (1982) hypothesized that because the baculum affects the shape of the penis, it acts during copulation by stimulating behavioral and neuroendocrine responses in females. This hypothesis is similar to the expected effects of cryptic female choice, although this term was coined later by Thornhill (1983) and popularized by Eberhard (1985)).

Interestingly, Patterson & Thaeler (1982) underscored a point made previously by Long & Frank (1968) and Long (1969), namely that the function of the baculum during copulation probably varies among species, given that the effect of the baculum on penis shape differs among species. For example, the penis of the Tayra (*Eira barbara*) matches closely with the shape of its baculum (Gonçalves *et al.*, 2022). In this species, as well as in other taxa in which the tip of the baculum protrudes beyond most soft tissues of the penis, there is more direct contact between the baculum and the females' vagina during copulation (Patterson, 1983). In contrast, in species such as the American pika (*Ochotona princeps*, Weimann *et al.*, 2014), the baculum is proximal to the tip of the penis and thus the latter probably interacts much less directly with the female's reproductive tract (see Patterson, 1983, for a discussion of baculum position in the penis of rodents). More recently, Schultz *et al.* (2016b) argued that the function of the baculum likely varies because it is not homologous among all lineages in which it is present, with multiple evolutionarily independent origins for this bone across the placental mammal phylogeny.

Currently, multiple studies have sought evidence for post-copulatory sexual selection driving the evolution of the baculum at different taxonomic levels and groups. Below I summarize some of these studies and, when possible, distinguish between sperm competition, cryptic female choice, and sexual conflict. However, differentiating among these processes is often not possible. I grouped studies depending on the type of data analyzed; namely functional morphology, interspecific comparative analyses, and experimental data.

Functional studies

Kelly (2000) described the histology of the penis of rats and revealed that the baculum is an extension of the corpora cavernosa (a high-pressure erectile tissue) and that they form one functional unit. A similar arrangement has been described for other species, including bats (Herdina *et al.*, 2010) and carnivorans (Enders, 1952). This organization of tissues implies that the baculum is responsible for transferring force in a way that increases the pressure within the corpora cavernosa, causing the penis to stiffen when force is applied to the tip, as likely happens during copulation (Kelly, 2000). Although this study suggests a mechanical function for the baculum during copulation, this function can be attained by

simple rod-shaped bacula. Thus, other processes are needed to explain the more complex shape exhibited by bacula.

Other studies have revealed functional aspects related to more complex features of bacula. For example, Herdina *et al.* (2015) showed that the baculum of some bats has a bifurcated proximal end. Images in 3-dimensions of artificially erected penises demonstrated that the bifurcated baculum protects the opening of the urethra, which may facilitate the delivery of sperm to the female vagina. In another functional study, Brassey *et al.* (2018) used 3-dimensional models of bacula and *in silico* tests of bending forces to demonstrate that the presence of a urethral groove in the baculum of carnivorans makes it more robust.

Comparative studies

Most variation in bacular morphology occurs among species, with morphologies being more uniform within species (Patterson & Thaeler, 1982). To understand the processes driving this variation, several studies have searched for correlations between bacular morphology and interspecific differences in reproductive strategies. In particular, comparative studies have focused on the relationship between baculum structure and 1) duration of copulation, and 2) mating systems and testis size.

Duration of copulation

In the first study to examine the association between bacular structure and aspects of reproductive behavior, Dixson (1987a) noted that relative baculum size correlated with duration of copulation in Primates. Specifically, primates with "long" copulatory durations tend to follow a higher allometric curve (*i.e.*, they have proportionally larger bacula) than those identified as having "short" copulatory durations. Later, Dixson (1995) reported a similar relationship for the Carnivora. Although these studies are suggestive, they were not conducted using phylogenetically informed methods that account for the non-independence of data from closely related species, thus the validity of the results is unclear. Nonetheless, in a more recent study using phylogenetically informed methods that also incorporate uncertainty in the phylogenetic relationships within primates and carnivorans, Brindle & Opie (2016) also found that species with larger bacula have "long" copulatory duration. It is important to note that these studies used a categorical definition for copulatory duration ("long" or "short"), which requires the choice of an arbitrary threshold for an otherwise continuous variable. When the length of the baculum and duration of copulation are treated as continuous variables in the Carnivora, the relationship is less clear: while Larivière & Ferguson (2002), did not recover a significant relationship, a study by Brassey *et al.* (2018) revealed a weak positive relationship between baculum length and duration of copulation (the latter study included a larger number of species). One challenge when using copulatory duration as a continuous variable is the difficulty to observe these events in animals' natural environments, and the data frequently come from a low number of observations or animals in captivity. Thus, this relationship may be further clarified with better data from more

species, but the current evidence suggests a weak positive correlation between the length of the baculum and copulatory duration. One possible explanation for this relationship is that a longer baculum assists sperm delivery by prolonging intromission after ejaculation (Dixson, 1987b; Larivière & Ferguson, 2002).

Nevertheless, baculum length is just one simple measurement. Brassey *et al.* (2018,2020) have looked for other aspects of the baculum of carnivorans that have a more clear functional correlation with duration of copulation. Specifically, using finite element analysis on 3D digital models of bacula, Brassey *et al.* (2018) were able to measure the robustness of the baculum to dorso-ventral bending forces applied to its tip. Robustness increases with features such as the overall dorsal curvature, dorsally curved distal tip, and the presence of a urethral groove (Brassey *et al.*, 2018). Further, these authors demonstrated a strong correlation between the robustness of the baculum and copulatory duration.

In another study, Brassey *et al.* (2020) quantified the complexity of bacula in 3-dimensions using the alpha-shapes summary statistic (Gardiner *et al.*, 2018). Although they did not find a correlation between the complexity of the entire baculum and duration of copulation in the Carnivora, they reported a weak positive relationship between the complexity of the distal tip and copulatory duration. Further, they found that the complexity of the baculum distal tip is higher in species with induced ovulation. Together, these results suggest that the baculum of carnivorans is associated with female stimulation during reproduction (Brassey *et al.*, 2020).

Mating system and Testis size

Dixson (1987b) showed that penile complexity is higher in primate species with social systems in which females have a higher chance of mating with more than one male. One of the variables that Dixson (1987b) used to categorize penile complexity was the length of the baculum, which tended to be longer in those mating systems. Although Dixson (1987b) used species-level analyses without considering their phylogenetic relationship, Verrell (1992) confirmed the previous findings at the level of genus, family, and using a "psedo-phylogeny" in an effort to take into account independent evolutionary events. The baculum of carnivorans also tends to be relatively longer in species with multi-male mating systems (Ferguson & Larivière, 2004, in a phylogenetically corrected analysis). However, Hosken *et al.* (2001) found a different result for bats. These authors reported a phylogenetic analysis in which baculum length was not correlated with mating system. Further, Hosken *et al.* (2001) investigated the relationship between baculum length and testes size, which is commonly used as an indicator for the degree of sperm competition (reviewed in Lüpold *et al.*, 2020), but again there was no correlation for bats. Given the lack of correlation between baculum length and both mating system and testes size, Hosken *et al.* (2001) concluded that the baculum of bats was not involved in sperm competition. Consistent with the different conclusions for different groups, Ramm (2007) demonstrated that this relationship varies among four mammalian orders. Although bats and primates do not have a correlation between testes' size and baculum length, both rodents and carnivorans have a positive correlation for these vari-

ables, and a positive correlation is also observed when the four orders are combined (Ramm, 2007). Similarly, Orr & Brennan (2016) reported that mammalian species with a baculum tend to have larger testis than those without a baculum. Interestingly, these authors also reported a positive (albeit weak) relationship between baculum width and testes mass, but no association between mating system and the presence of bacula.

Perhaps the clearest indication that mating systems can affect the evolution of the baculum has been observed in the order Carnivora overall as well as in one of its subclades, the pinnipeds. The 3D morphological complexity of the baculum of carnivorans correlates significantly with the mating system (Brassey *et al.*, 2020). Further, the rate of evolution of 3D bacular complexity is slowest in socially monogamous species, slightly faster in solitary species, and fastest in species in which multiple females live in groups (Brassey *et al.*, 2020). Similarly, pinniped species that form harems have a faster rate of evolution for the length of the baculum than those without harems (Fitzpatrick *et al.*, 2012). Further, pinnipeds display a positive correlation between the length of the baculum and testis mass (both corrected for male body mass, Fitzpatrick *et al.*, 2012), but this correlation is much weaker in the Carnivora (Brassey *et al.*, 2020), which suggests that the baculum plays a more important role in sperm competition in pinnipeds than other carnivorans. Interestingly, Fitzpatrick *et al.* (2012) found that species with harems have more sexual size dimorphism, relatively shorter bacula, and smaller testes. Thus, these authors suggest that there is a trade-off between pre- and post-copulatory sexual selection, in which more investments in pre-mating male-male competition strategies (expressed by male size) are negatively correlated with investments in post-mating characters (baculum and testes size). The observation that the length of the baculum correlates with both testis size and mating systems suggests that the baculum is involved in sperm competition.

Considering a scenario of cryptic female choice acting on the baculum, Kinahan *et al.* (2008) suggested that baculum size may be an indicator of a male's genetic quality, such that females would favor males with larger bacula. Specifically, these authors predicted that species with multi-male mating systems would have positive allometric slopes (*i.e.*, larger males would have a proportionally larger baculum than smaller males of the same species), but either isometry or negative allometry would be expected for the baculum of species in which females mate with a single male. Although positive allometry was recovered for the baculum of one species of African mole rat with a multi-male mating system (Kinahan *et al.*, 2007), a comparison with other three species in the same family (Bathyergidae) did not find the predicted relationship between allometric slope and mating system (Kinahan *et al.*, 2008).

Experimental studies

The relationship between baculum morphology and differential reproductive success has been examined experimentally in house mice. Using a design in which multiple individuals shared large outdoors enclosures, Stockley *et al.* (2013) demonstrated post-copulatory sexual selection given that males with a wider base of the baculum had significantly more offspring

per litter than males with narrower bacula. Thus, the higher fitness of males with wider bacula implies directional selection towards wider bacula in house mice. This prediction was confirmed in an experimental evolution setup in which the width of the base of the baculum increased after 27 generations of mice kept in a laboratory environment with risk of sperm competition, while this correlation was not observed in mice maintained without risk of sperm competition (Simmons & Firman, 2014). Although the width of the baculum also increased plastically when mice were reared in conditions of sperm competition (André *et al.*, 2018), it is important to note that the morphological variation of the baculum shape (especially its width) does have a component of heritable additive genetic variation (Schultz *et al.*, 2016a; André *et al.*, 2020b). This indicates that the baculum of house mice can evolve in response to (sexual) selection, consistent with Simmons & Firman (2014) observations. However, selection on the baculum of house mice is not simply towards a wider morphology. An experiment that demonstrated more subtle effects of baculum shape on male fitness used a design in which females were paired with two males consecutively (André *et al.*, 2020a). These authors found that the percentage of embryos with paternity assigned to the second male depended on an interaction between bacular morphology and the female lineage. In another experiment, André *et al.* (2021) reported that female mice responded differently to male stimulation depending on the interaction between bacular morphology and male copulatory behavior (female response was measured by prolactin hormone levels after copulation). In summary, recent experiments have shown that the width of the base of the baculum of house mice responds to increased risks of sperm competition (Stockley *et al.*, 2013; Simmons & Firman, 2014), however, its effects on female stimulation depend on the females' genetic lineage and males' copulatory behavior (André *et al.*, 2020a, 2021).

1.3 Dissertation objectives

The increasing number of recent studies on the baculum has greatly improved our understanding of the role that this bone plays in the reproduction of mammals, especially given that the baculum is correlated with multiple aspects of their reproductive strategies. It is worth noting that it is unusual for a structure associated with the reproductive system of animals to be made of hard tissues such as bones, but this characteristic makes the baculum a structure of interest for vertebrate paleontology. As a bone, the baculum has a much higher potential for fossilization than structures associated with the genitalia of most animals. In this dissertation, I explore this feature to study the evolution of the baculum of the Canidae comparing extinct and extant species.

The family Canidae is subdivided into three subfamilies: the extinct Hesperocyoninae and Borophaginae, and the extant Caninae. These three subfamilies have an abundant and diverse fossil record, particularly in North America (Wang, 1994; Wang *et al.*, 1999; Tedford *et al.*, 2009). However, very few fossils of the baculum of canids have been studied, and only one study has made inferences for the reproductive biology of an extinct canid (Hartstone-Rose *et al.*, 2015).

In Chapter Two, I describe the bacula of five extinct species of Borophaginae, each of which was found with other skeletal elements that have enabled identification to the species level. Two specimens (*Aelurodon ferox* and *Aelurodon stirtoni*) are largely complete, while the baculum from *Carpocyon compressus* is complete but still embedded in matrix that obscures some of its features. The bacula of *Paratomarctus euthos* and *Desmocyon thomsoni* are incomplete, but they provide useful information nonetheless. These borophagine bacula are similar to extant canines in being robust, having a urethral groove, and a simple distal end. These features suggest that the Borophaginae had long-lasting copulation and possibly spontaneous ovulation, similar to the extant canines. However, unlike the straight baculum of extant canines, borophagine bacula are ventrally curved (arched), which is also observed in the hesperocyonine baculum.

In Chapter Three, I examine the intra- and interspecific 2D variation in the morphology of the baculum of canids using elliptic Fourier analysis. Extant canids have a distinctive baculum, exhibiting large intraspecific variation with generally small differences among species. This makes it difficult to distinguish between many of the canid species and even genera based on their bacular morphology. Nonetheless, some species can be diagnosed, for example, the gray fox. Within the Caninae, the extinct dire wolf (*Aenocyon dirus*) is also easily distinguished based on size and shape. While the baculum of extant canids is mostly straight, bacula from the two extinct subfamilies, the Hesperocyoninae and Borophaginae, have a distinctive arched morphology. Because these fossil taxa are closer to the root of the canid phylogeny they have a larger effect than the extant species on the reconstruction of the ancestral state of the entire family; I show that there is only a small probability that the arched morphology was ancestral for the entire family based on the analysis of extant species alone, but that the inclusion of fossils strongly indicates that an arched baculum was ancestral. Thus, the fossils indicate that the straight baculum of extant species evolved in the stem group of the canines, between ∼40 and 12.5 Ma. Understanding the functional differences between arched and straight bacula may offer insight into the selective pressures that led to the unique bacular structure of canines.

In Chapter Four, I explore the allometric relationship between baculum length and body size in canids. Examination of 26 (out of ∼35) extant species using phylogenetic generalized least squares revealed a slightly negative allometric slope of around 0.91; but this value was indistinguishable from one, indicating that isometry is possible. Within the Caninae the baculum of the extinct dire wolf (*Aenocyon dirus*) is significantly longer than expected based on its body size, raising the possibility that its reproductive biology might have differed from extant canines. Two complete bacula are known from the borophagines (*Aelurodon ferox* and *A. stirtoni*), both of which fall on the same allometric relationship as the living canids (although they have a distinctive shape). However, the only known hesperocyonine with a preserved baculum, *Hesperocyon gregarius*, deviates from the allometric relationship found in living canids, showing a proportionally much longer baculum, as well as a distinctive shape.

Chapter 2

Fossil bacula of five species of Borophaginae (Family: Canidae): implications for their reproductive biology

2.1 Introduction

Studying the reproductive biology of extinct animal groups is challenging. While neontologists can observe directly the morphology, behavior, endocrine responses, and life cycles of their study organisms, it is extremely rare for paleontologists to find direct evidence of reproductive biology (*e.g.* a fossilized pair of mating insects Fischer & Hörnig, 2019). Instead, paleontologists must rely largely on morphological traits that fossilize, and on the fidelity of correlations between these traits and other aspects of reproduction seen among extant species. As a result, we have much less information regarding the reproductive biology of extinct species than for living species. Consistent with this, sexual selection and mating represent less than 5% of all the entries in the compendium of behaviors inferred from fossils (Hsieh & Plotnick, 2020, tabulated Boucot & Poinar Jr., 2010's compendium). Nonetheless, when aspects of reproductive biology can be inferred, they can provide important insights into observed changes in biodiversity. For example, Bush *et al.* (2016) showed that marine animals with direct fertilization drive the diversification of marine fauna during the Cretaceous-Cenozoic while groups that spawn in the water column have a relatively constant diversity over the same period.

In this context, the penis bone of mammals (baculum, *os penis* or *os priapi*) provides an opportunity for drawing inferences regarding the reproductive biology of extinct species (*e.g.*, Abella *et al.*, 2013). The baculum is present in 7 mammalian orders, within which it has been gained and lost multiple times (Schultz *et al.*, 2016b). Interestingly, females of some species have *ossa genitalia* homologous to the baculum, the baubellum or *os clitoridis*,

but it is normally smaller than the male counterpart (*e.g.,* Spani *et al.*, 2021) and is largely understudied, to such an extent that it has not been associated with any aspect of animals' reproductive biology. The baculum can inform our understanding of the reproductive biology of extinct species because it is a part of the male genitalia with potential for fossilization and because its morphology is known to correlate with several aspects of the reproductive biology of extant mammals. For example, in carnivorans, induced ovulation tends to occur in species that have bacula with a more complex distal tip (Brassey *et al.*, 2020). Moreover, more robust bacula are associated with prolonged copulation (Brassey *et al.*, 2018), and longer bacula are associated with larger testis (Ramm, 2007; Brassey *et al.*, 2020), which is indicative of stronger sperm competition (Lüpold *et al.*, 2020).

A good fossil record for carnivoran bacula would allow us to explore how the reproductive biology of this mammalian clade has changed through time. However, very few extinct species have had bacula described (but see Hatcher, 1902; Peterson, 1910; Olsen, 1959; Harrison, 1982; Wang, 1994; Dundas, 1999; Abella *et al.*, 2013, the the description of the baculum in eight species). To date, bacula have only been described from two extinct canid species: *Hesperocyon gregarius* in the extinct subfamily Hesperocyoninae (Wang, 1994), and the dire wolf, *Aenocyon dirus* (Dundas, 1999; Hartstone-Rose *et al.*, 2015), in the still extant subfamily Caninae. Here, I add to our knowledge of canid bacula by describing the bacula of five species of Borophaginae, the other extinct subfamily of Canidae. All specimens are from North America and were found associated with sufficient other skeletal elements to allow identification to the species level. These are the first descriptions of bacula that can be reliably attributed to Borophaginae.

The subfamily Borophaginae has a rich fossil record, spanning over 30 Ma, from the Orellan (base around 34 Ma, early Oligocene) to the Blancan (top around 1.8 Ma, early Pleistocene) with at least 66 recognized species (Wang *et al.*, 1999). They were the most diverse group of carnivores in the middle Miocene in North America (Silvestro *et al.*, 2015), and by that time had radiated from a small hypocarnivorous ancestor to exhibit a diverse range of body sizes and diets (Slater, 2015). Functional morphological studies have led to opposing conclusions regarding whether they formed groups to hunt or not (Van Valkenburgh *et al.*, 2003; Andersson, 2005). Currently, very little is known about their reproductive biology – the bacula described here offers new insights into this aspect of their biology.

2.2 Bacula of extant canids

I use the bacula of the extant canids (all from subfamily Caninae, Didier, 1948; Hildebrand, 1951; Burt, 1960) as a reference for the anatomy of Borophaginae bacula. Most extant canines have a fairly straight baculum in lateral profile, although it may curve slightly ventrally (concave down) or dorsally (concave up). On the ventral side, there is a deep groove that runs from the proximal end to about three-quarters down the length of the shaft. The urethra sits within this groove. The presence of the groove is associated with lateral expansions of the baculum along its ventral margin, which also results in a distinctive proximo-

distal dorsal crest. Most individuals have a peak somewhere along the proximal-half of the dorsal crest, but it is absent in some specimens. The proximal end of the baculum shows marks of soft tissue attachment (scars). The distal end (anterior) is simple, having either a cylindrical rod-like shape or being slightly expanded dorso-ventrally. The cartilaginous distal-most portion of the baculum, the apex, can calcify with age (Hildebrand, 1951) but is rarely observed in zoological collections.

2.3 Descriptions of borophagine bacula

Museum Abbreviations: F:AM – Frick Collection, Department of Vertebrate Paleontology, American Museum of Natural History, New York, NY; USNM PAL – Smithsonian Institution National Museum of Natural History Paleontology collections, Washington, D.C.; UNSM – University of Nebraska State Museum, Lincoln, NE.

Paratomarctos euthos

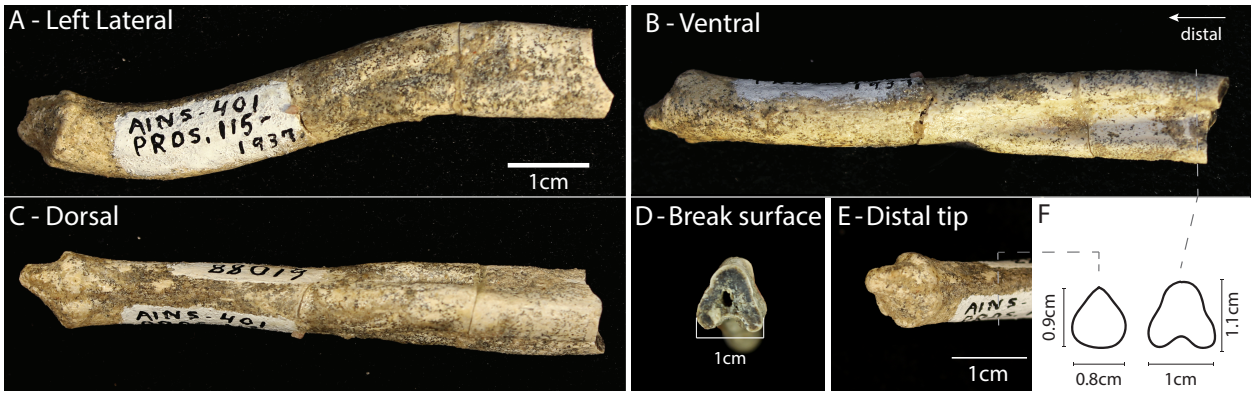

Figure 2.1: The partially preserved baculum of *Paratomarctos euthos* (F:AM 61088), exhibiting the complete distal end. A) Left lateral view showing the sigmoidal profile of the bone. B) Ventral view showing the beginning of the ventral groove about halfway down the specimen, which then expands proximally. C) Dorsal view showing the lateral expansion where the ventral groove is present and the resulting dorsal crest. A,B and C are at the same scale; anterior at left. D) Slightly oblique view of the broken end. E) Oblique view of distal tip. F) Inferred cross-sections at two points along the specimen.

The distal portion of the baculum of *Paratomarctus euthos* (Figure 2.1) was found associated with fragments of the skull and mandible as well as numerous post-cranial bones (specimen F:AM 61088 – Wang *et al.*, 1999). This specimen is from the late Clarendonian (13.6-10.3Ma, middle Miocene) from the Merritt Dam Member of the Ash Hollow Formation, Cherry Co., Nebraska. The preserved portion of the baculum is 7cm long. Despite

the absence of the proximal end, it is clear that the baculum was robust. The ventral side of the proximal portion exhibits a shallow and wide urethral groove, with a corresponding dorsal crest. Moving distally, the groove becomes gradually shallower and narrower until it disappears about halfway along the preserved portion of the baculum. The distal end consists of a small conical projection of rough bone. At the base of this cone there is an almost continuous circumferential ring of bone. The baculum is sigmoidal in lateral profile. There is an overall ventral curvature (concave down) that changes to a dorsal curvature (concave up) at the distal third of the specimen. Given the aspect ratio (length to width) of the specimen it seems likely that the fragment represents at least 50% of the total length of the baculum.

Desmocyon thomsoni

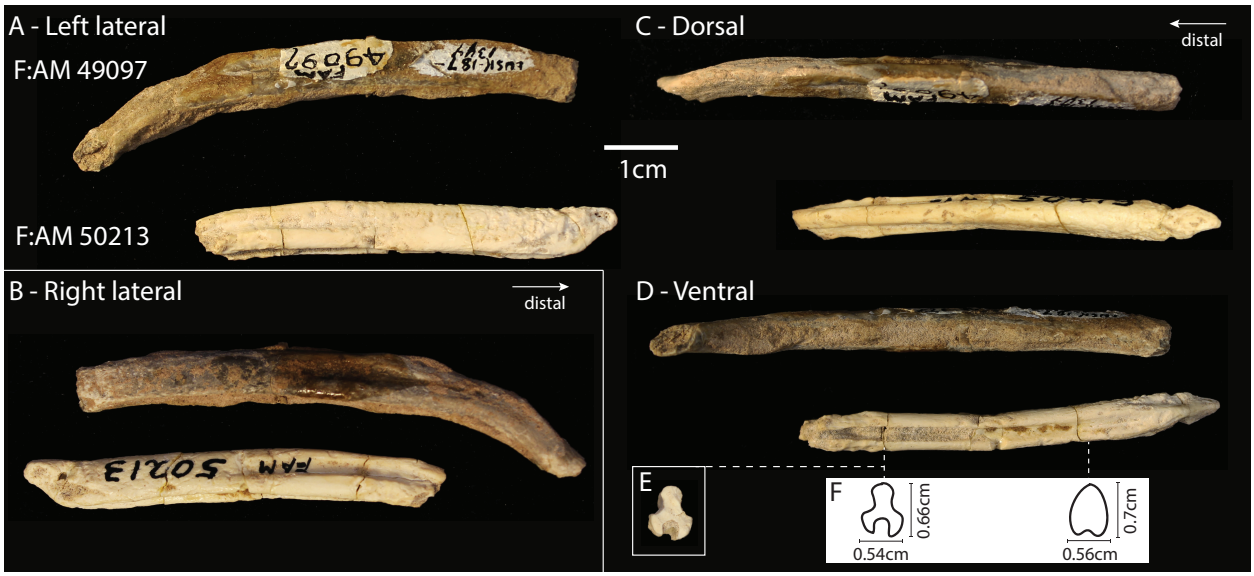

Figure 2.2: Bacula of *Desmocyon thomsoni* from specimens F:AM 49097 (upper image in each panel) and F:AM 50213 (lower image in each panel). In each panel the specimens are roughly aligned based on the proximal ends of the dorsal crest — it appears that F:AM 49097 is only missing a small portion of its proximal end, while F:AM 50213 is missing a larger portion of its distal end. A) Left lateral view, showing the ventral curvature in F:AM 49097 and soft tissue attachment marks on the proximal end of F:AM 50213. B) Right lateral view. The right side of specimen F:AM 49097 is less abraded giving a better view of the dorsal crest, which is absent from the proximal and distal ends. C) Dorsal view shows the dorsal crest of both specimens, and the triangular distal end of F:AM 50213. D) Ventral view showing the urethral groove in both specimens, although it is filled with matrix in specimen F:AM 49097. The distal surface for this specimen also shows that the specimen broke distally to the distal end of the groove. E) Cross section of the baculum F:AM 50213 where there is a clean break in the specimen. F) Inferred cross sections with caliper measurements indicated.

Two partial bacula of *Desmocyon thomsoni* (Figure 2.2) are associated with partial skeletons, including partial skulls and mandibles as well as many elements of the post-crania skeletons (Wang *et al.*, 1999). Both are from the late Arikareean (30.8 – 20.43Ma, Oligocene-Miocene) of Wyoming. Specimen F:AM 49097 was found in the Lusk area, Upper Harrison beds in Goshen Co., Wyoming. Specimen F:AM 50213 is also from the Lusk area, Upper Harrison beds, but in Niobrara Co., Wyoming.

Specimen F:AM 50213 has a complete proximal end where marks of soft tissue attachment are present on the lateral surface. The marks form a 1.5 cm long diagonal line that extends from the dorsal and proximal extremity to the ventral face of the shaft. On the lateral surface, and dorsal to this diagonal line, the bone is rougher but transitions to smoother bone distally. The fragment is mostly straight in lateral profile, except for a slight ventral curvature that starts about one centimeter from the broken end of the specimen. In ventral view there is a deep urethral groove that is narrow and cylindrical. The proximal end of the baculum is laterally compressed, corresponding to where the urethral groove disappears. This differs from most modern canids, in which the urethral groove extends all the way to the proximal end, but is similar to the baculum of the gray fox, *Urocyon cinereoargenteus* (Burt, 1960). The dorsal surface of the baculum presents a strong proximal-distal crest, which can be seen clearly in the cross-section of the broken surface (Figure 2.2E).

Specimen F:AM 49097 is slightly longer than F:AM 50213 (6.9 cm and 5.63 cm, respectively), but it is more abraded and is missing both the proximal and the distal ends. This specimen preserves more of the distal end than F:AM 50213, revealing a ventral curvature (concave down). The groove is not visible on either the proximal or distal broken surfaces and is thus restricted to the middle portion of the bone; it is filled with sediment, which obscures the ends of the groove. The dorsal crest is present in the middle portion of the fragment, but not at the proximal and distal ends. Using the proximal end of the crest and the lack of the urethral groove on the proximal break surface as reference points to align the two specimens, it is possible to infer that only a small portion of the proximal end of F:AM 49097 is missing. It is not possible to see where the groove ends distally due to sediment and abrasion, but the groove is not present on the distal break surface (as visible in Figure 2.2D). The specimen starts to taper distally and the dorsal crest is not present along the distal portion. Given these features of the distal portion and given that other canid bacula have fairly simple distal ends, it seems likely that only a small fraction of the distal end of this specimen is missing.

Aelurodon ferox

One baculum of *Aelurodon ferox* was found together with a partial skeleton, specimen F:AM 61723, which has a partial mandible and numerous postcranial bones (Wang *et al.*, 1999). The specimen is considered Clarendonian in age (13.6-10.3Ma, middle Miocene), from the Pojoaque Member of the Tesuque Formation (Santa Cruz Grant, Santa Fe Co., New Mexico).

Figure 2.3: The baculum of *Aelurodon ferox* (F:AM 61723). A) Dorsal view: showing the lateral expansion on the middle part of the shaft where the ventral groove is present. B) Lateral view showing the ventral curvature and the tapering of the bone distally. C) Ventral view showing the urethral groove. The same scale applies to A, B and C. D) Closer view of the distal tip (1cm scale bar). E) Inferred cross-sections at four points along the bone with caliper measurements indicated.

While Wang *et al.* (1999) mentioned the presence of a "partial baculum", the specimen appears to be mostly complete, missing only a minimal portion of the proximal end. It is a robust bone measuring 11.7 cm in length. When observed in lateral view, it curves ventrally and tapers distally (Figure 2.3). Soft tissue attachment scars are not visible at the proximal end, although the bone seems slightly rougher at that end. A urethral groove is not visible at the proximal end, but begins about 2cm from the proximal end and becomes deeper until about two-thirds along the shaft, where it again becomes shallow until it disappears where the distal curvature becomes strongest. Where the groove is present, there is a lateral expansion of the lower (ventral) half of the bone which leaves the dorsal crest visible. The dorsal (and ventral) view reveals that the proximal end is laterally compressed where the groove is absent. The distal end is almost cylindrical in cross-section. The distal face of the distal end shows rougher bone, similar to some modern canids.

Aelurodon stirtoni

The baculum of specimen USNM PAL 215320 (Figure 2.4) was found with an almost complete skeleton as well as a partial skull and mandible with all teeth preserved (Wang *et al.*, 1999). It is from the late late Barstovian (15.97-13.6Ma, middle Miocene) and was found in the Burge Member of the Valentine Formation, Cherry Co., Nebraska (Wang *et al.*, 1999). Although several parts of the skeleton have already been described and imaged (Munthe, 1989), the baculum has not. My description of the baculum is based on pictures provided by the Smithsonian National Museum of Natural History. The specimen is on display at that museum and the mount added to position the baculum obscures the dorsal side of the proximal end.

The specimen is complete and has a simple shape. In lateral profile it curves ventrally, showing little variation in dorso-ventral height along the shaft. On the ventral side a shallow groove is present along most of the shaft, disappearing just before the proximal and distal ends. In contrast to the bacula described above, the baculum in this species lacks the lateral expansions typically associated with the urethral groove, and thus there is no dorsal crest. The proximal end is triangular and displays rougher bone that is typically associated with soft tissue attachment. The distal end has an approximately circular circumference (although slightly pinched on the dorsal side) and consists of rough and porous bone.

Carpocyon compressus

This specimen (UNSM 128864, Figure 2.5) was found in association with a partial skeleton and complete skull and mandible (Wang *et al.*, 1999, where they refer to the specimen field number UNSM 2556-90). It is late Barstovian (15.97-13.6Ma, middle Miocene), from the Valentine Formation, Brown County, Nebraska (Wang *et al.*, 1999). Here I describe the baculum based on photographs provided by the University of Nebraska State Museum. The baculum is partially embedded in matrix along with other post-cranial bones.

Figure 2.4: The baculum of *Aelurodon stirtoni* (USNM PAL 215320). The dashed area indicates material added to the specimen so that it could be mounted as part of an exhibit. A) Dorsal view, which indicates the lack of a lateral expansion seen in other species where the urethral groove is present. The mount obscures details of the proximal end. B) Left lateral view showing the ventrally curved profile. C) Ventral view showing the presence of a shallow groove along most of the length of the shaft but that disappears at both the distal and proximal ends. D) View of the distal end. There was insufficient information to infer cross-section shapes. Images courtesy of the Smithsonian Institution.

The specimen appears to be complete but has one break close to the proximal end. This break slightly alters the lateral profile, but a ventral curvature is clear. The ventral side contains a deep urethral groove that extends for almost the entire length of the bone, ending about 1 cm before the distal end and about 1 cm from the proximal end. Although the dorsal side is still embedded in matrix, in lateral view lateral expansions associated with the groove can be seen, as can the corresponding dorsal crest. The matrix covering the proximal end makes it difficult to determine if there were any soft tissue attachment scars. The distal tip is laterally compressed but has a height similar to the height along most of the shaft. This is in contrast to most canid bacula, which tend to show compressed and cylindrical distal ends.

Figure 2.5: The baculum of *Carpocyon compressus* (UNSM 128864). A) Ventral view showing a deep urethral groove. B) Right lateral view, with the ventral side facing up on the picture, showing the baculum's ventral curvature. C) Distal end in left lateral view. There was insufficient information to infer cross-section shapes.

2.4 Discussion

The bacula of the five borophagine species described here display similarities to each other and to the bacula of all other canids. Specifically, the bacula of extant canines, the extinct hesperocyonine *H. gregarius*, and borophagines are similar in terms of: *i*) relatively large size; and, *ii*) a ventral urethral groove along much of the length of the shaft but not at the distal tip. In two traits the five borophagine bacula are similar to *H. gregarius* but differ from the extant canines: *i*) their ventral curvature (concave down) in lateral profile; and *ii*) the closed urethral groove at the proximal end. Finally, the simple and mostly straight distal end of borophagine bacula is similar to extant canids but differs from the up curved

"hook-like" distal end of *H. gregarius*' baculum (Wang, 1994). Figure 2.6 shows lateral view silhouettes of these bacula for comparative purposes, with examples of bacula of species in other families to capture some of the variation of bacular morphology. Below I discuss how morphological features of borophagine bacula may have implications for their reproductive biology.

Relative size

Similar to modern canids, the bacula of the Borophaginae were large and robust bones. This supports the observation from Wyss & Flynn (1993) that a large baculum is generally diagnostic for the Suborder Caniformia (which includes Canidae, Ursidae, Musteloidea, Pinnipedia, and Amphicyonidae) and contrasts with the generally reduced bacula of the sister group, the Feliformia.

Implications for reproductive biology

Several studies have explored the relationship between baculum length and the reproductive biology of the living carnivorans (*e.g.*, Dixson, 1995; Ramm, 2007; Larivière & Ferguson, 2002; Fitzpatrick *et al.*, 2012; Brindle & Opie, 2016; Brassey *et al.*, 2018, 2020). These relationships can thus be used to draw inferences about the reproductive biology of the Borophaginaes. From a functional standpoint, the baculum adds rigidity to the erect penis, therefore the longer and more robust it is, the more it can aid in the maintenance of long-lasting copulations. For example, extant carnivoran species with long-lasting copulations (defined as more than 3 minutes) tend to have longer bacula (whether phylogeny is considered Brindle & Opie, 2016, or not Dixson, 1995), but this relationship is not significant when using duration of copulation as a continuous character (Brassey *et al.*, 2018; Larivière & Ferguson, 2002).

Among extant carnivorans, there is a weak correlation between longer bacula and larger testis mass, when both body mass and phylogeny are accounted for (Ramm, 2007; Fitzpatrick *et al.*, 2012, but see Brassey *et al.*, 2020, who found just a weak signal for this relationship). Larger testis mass is frequently interpreted as a good indicator of the strength of sperm competition because increased sperm production increases the chances of fertilization when females may mate with more than one male during a single round of reproduction (reviewed in Parker & Pizzari, 2010; Lüpold *et al.*, 2020).

Both of these relationships — copulatory duration and likelihood of sperm competition — suggest that the baculum plays a role in postcopulatory sexual selection, especially in species in which longer copulations may function as a form of mate-guarding that prevents a female from mating with additional males (Alcock, 1994) and/or greater sperm production to increase the odds of paternity over competitors. Given that these mechanisms of postcopulatory sexual selection are correlated with large bacula, the relatively large size of bacula within the Borophaginae suggests that similar mechanisms may have been present in these extinct taxa. Given the limited sample size for the Borophaginae and the relatively weak

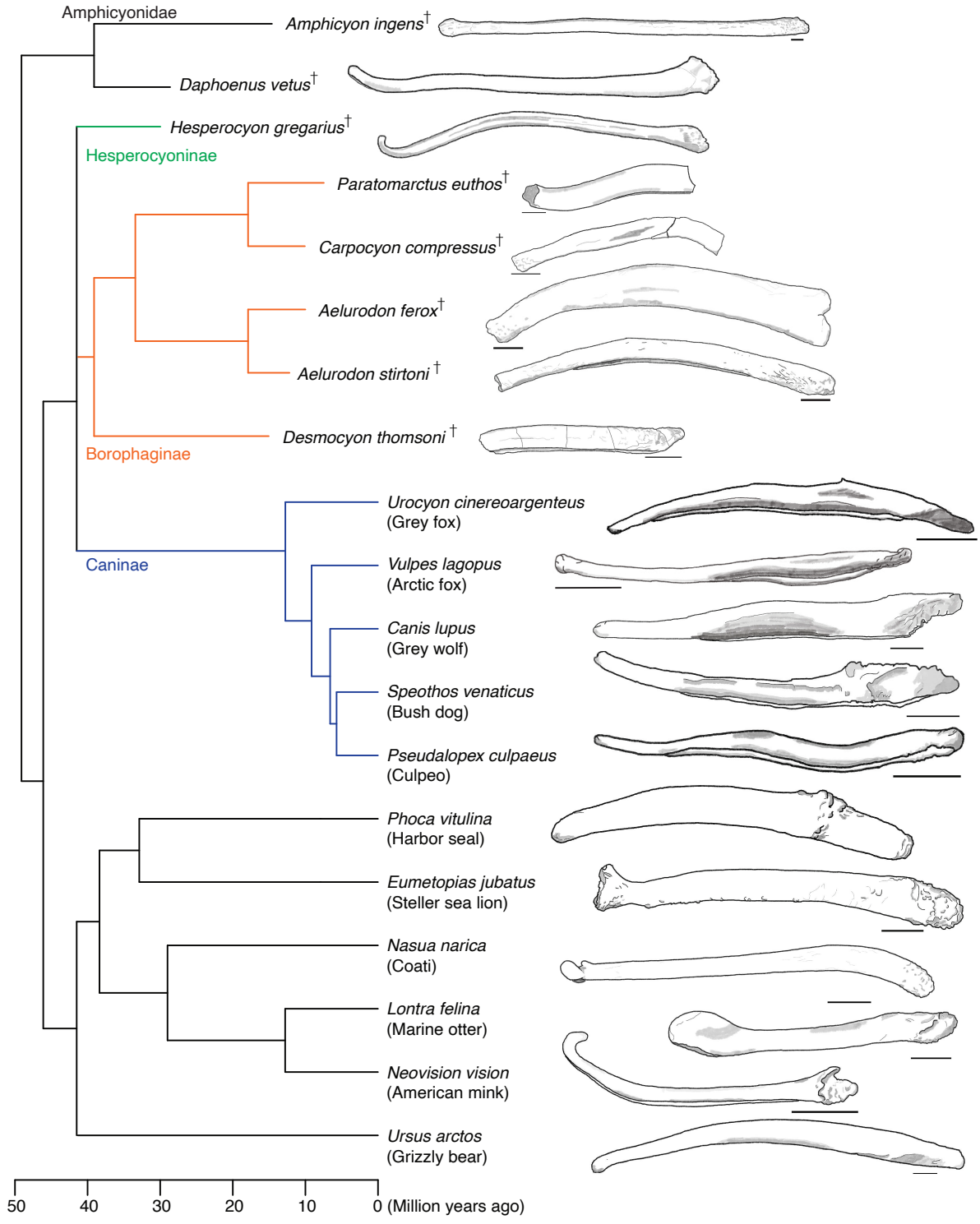

Figure 2.6: Lateral view silhouettes of bacula of borophagines and selected species [continues]

Figure 2.6: within the suborder Caniformia. The specimens represented were chosen to illustrate a substantial range of morphological variation of the canid bacula as well as a few representative morphologies observed in other families. For further examples of morphological variation of bacula refer to Didier (1948); Burt (1960); Baryshnikov *et al.* (2003). Drawings for the Borophaginae are based on photographs in this paper (above). Silhouettes from extant species are based on specimens observed at the Museum of Vertebrate Zoology, Berkeley, California. Drawings from extinct species are based on published images for *Amphicyon ingens* (Olsen, 1959), *Daphoenus vetus* and *Hesperocyon gregarius* (Scott & Jepsen, 1936). The underlying phylogeny is for illustrative purposes and it is based on: Slater (2015) for the relationship between the Borophaginae, Caninae and Hesperocyoninae; Slater & Friscia (2019) for the position of Ursidae (grizzly bear), Mustelidae (marine otter and American mink), and Procyonidae (coati); Paterson *et al.* (2020) for the position of Pinnipedia; and Tomiya & Tseng (2016) for the position of the extinct Amphicyonidae (*Amphicyon* and *Daphoenus*). Time scale in million years ago, with ranges of extinct species projected to last fossil occurrences of the taxon.

---

relationships between baculum length and these aspects of postcopulatory competition in extant carnivorans (Brassey *et al.*, 2020), I have refrained from using these relationships to estimate actual values for copulatory duration and testis mass for the Borophaginae.

Urethral groove

The urethral groove is present in all bacula described from canids, including *H. gregarius* (Wang, 1994), the borophagine specimens examined here, as well as the extant and extinct canines (Didier, 1948; Hildebrand, 1951; Burt, 1960; Hartstone-Rose *et al.*, 2015). This suggests that this trait is plesiomorphic for the family.

Interestingly, a groove is also present in other families within the Suborder Caniformia, including the extinct and basal Amphicyonidae (Olsen, 1959; Peterson, 1910), some mustelids, and pinnipeds. Canids, however, appear to have a unique configuration of the urethral groove. Based on published descriptions (*e.g.*, Didier, 1948; Burt, 1960) and my own observations of the bacula of the other caniform families, the canids appear to be the only taxon in which the urethral groove is deep, runs for most of the length of the baculum, and is absent at the distal end. While the configuration of the canid urethral groove appears to be unique, it does show variation, mostly in its depth, width, and whether it terminates before the proximal end or not. For example, the groove of *Aelurodon* is shallower than in other canids.

In contrast, in the members of other carnivoran families that have a deep groove, the groove continues to the distal-most tip of the baculum, and may even be restricted to the distal tip, for example, extant otters (*Lontra*, *Lutra*, and *Pteronuria*), weasels (*Mustela*), and bearded seals (*Erignathus barbatus*) (personal observation). The deep distal groove

is also observed in two fossil bacula described from the Amphicyonidae (*Amphicyon ingens* and *Daphoenus*, Olsen, 1959; Peterson, 1910, respectively), a stem family of the Caniformia (Tomiya & Tseng, 2016). Finally, some bears (Family Ursidae – *e.g.*, spectacled bear *Tremarctos ornatus*, and polar bear *Ursus maritimus*, personal observation) have a urethral groove in a similar position (on the middle of the shaft, absent at the distal end), but much shallower than that of canids.

Finally, while most canine species have an open urethral groove at the proximal end (*e.g.*, Burt, 1960), there are two exceptions, the gray fox (*Urocyon cinereoargenteus* – Burt, 1960) and the bat-eared fox (*Otocyon megalotis* – personal observation), both of which are more similar to the borophagine condition of having a closed proximal end. Interestingly, the gray fox is the most basal species in phylogenetic reconstructions of canines that include fossils (*e.g.,* Zrzavý *et al.*, 2018, but see Lamarca & Schrago, 2020, for a discussion of the position of the root of extant canids phylogeny), suggesting that the transition from a closed to an open proximal end might have occurred within the Caninae.

Implications for reproductive biology

It has been suggested that the urethral groove protects the urethra during copulation, facilitating the delivery of sperm (Dixson, 1995). Functional experiments support this inferred function in some bats (Herdina *et al.*, 2015), although the shape and position of the groove in these species are different from that of canids. *In silico* functional models of grooves more similar to those seen in canids (Brassey *et al.*, 2018) have demonstrated that the groove increases the robustness of bacula subject to dorso-ventral forces. Given this result, and given that robustness is correlated with long-lasting copulations (Brassey *et al.*, 2018), it seems likely that a reinforced baculum with a urethral groove that aided in the delivery of sperm and enabled prolonged copulation was the ancestral to the divergence of the three subfamilies of canids.

The presence of a urethral groove may also have implications for borophagine mating systems. The urethral groove is a major contributor to bacula complexity when its morphology is quantified from 3D digital scans (Gardiner *et al.*, 2018; Brassey *et al.*, 2020). Brassey *et al.* (2020) found that socially monogamous species tend to have bacula that are slightly more complex than solitary species, while species that live in groups with several breeding females tend to have bacula less complex than the other two mating systems. If this relationship also applies to the borophagines then their deep urethral groove would suggest that they did not have a mating system with multiple breeding females, although this inference remains tentative.

Distal end

The distal end of the borophagine baculum shows a simple morphology, either mostly cylindrical or laterally compressed, which is similar to the simple distal end observed in extant canids (Burt, 1960). In contrast, the extinct hesperocyonine *H. gregarius* had a

dorsally-curved distal tip (Figure 2.6, Wang, 1994; Scott & Jepsen, 1936), which is much more complex than other known canid bacula and more similar to that of some extant mustelids and procyonids.

Implications for reproductive biology

The distal end of the baculum of extant carnivorans is associated with the mode of ovulation. While species with more complex distal tip tend to show induced ovulation, those with simple distal tips are associated with spontaneous ovulation (Brassey *et al.*, 2020). Given that most extant canids have spontaneous ovulation, the bacula described here suggest a similar strategy for the borophagines. Larivière & Ferguson (2003) hypothesized that induced ovulation is advantageous for species with low population densities and with a multi-male mating system that live in highly seasonal environments (see also Heldstab *et al.*, 2018). Although their hypothesis does not entail that high population densities are associated with spontaneous ovulation, species with higher population density have higher chances of mate encounters during the restricted time window of spontaneous ovulation. The fossil record of borophagines is particularly rich (Van Valkenburgh *et al.*, 2003), consistent with the potential for high population densities in these animals. Together with the bacular structure of these animals, available evidence, although limited, suggests that the borophagines were spontaneous ovulators.

Curvature

All bacula described here have a primarily ventral curvature (arched) in lateral profile (Figure 2.6), with one species (*P. euthos*) having a secondary dorsal curvature on the distal end. Only two specimens (both *Aelurodon*) have complete bacula without any indication of preservational distortion (such as bending or warping), while for the other three species the bacula are either incomplete or had the lateral profile slightly altered by a break (*C. compressus*). Nevertheless, a primarily ventral curvature is seen in all specimens. In this regard, the bacula of the Borophaginae differ from the mostly straight or even dorsally curved bacula of almost all extant canids (Figure 2.6). For the very few extant canids (such as the gray fox) with a ventrally curved baculum, it is not as curved as in *Aelurodon*. The degree of ventral curvature in the borophagines is present in some bears and pinnipeds, although more data are necessary to establish the generality of this observation.

Implications for reproductive biology

Using *in silico* biomechanical analyses, Brassey *et al.* (2018) showed that a ventral curvature leads to less robust bacula when a dorso-ventral force is applied to its distal tip. In turn, species with less robust bacula show a shorter duration of copulation (Brassey *et al.*, 2018). Based on this feature alone, it is possible to hypothesize that the baculum of borophagines would not withstand as much force during copulation as modern canids and thus had a

shorter duration of copulation than extant canids. However, other morphological features may have increased the robustness of the borophagine baculum, which would suggest a long copulatory duration. For example, the baculum of *Aelurodon ferox* (Fig. 2.3) is a massive bone, with a thick dorsal ridge and a dorso-ventral height that is larger than observed in modern carnivorans. Further quantitative analysis similar to those of Brassey *et al.* (2018) should help clarify the robustness of borophagine bacula, and thus inferences about their copulatory duration.

2.5 Conclusion

The baculum of borophagines shows an overall similarity with extant canines in relative size, a simple distal end, and the presence and configuration of a urethral groove. Drawing upon correlations between bacular morphology and reproductive biology of the extant canids, it is possible to generate preliminary inferences regarding some aspects of borophagine reproductive biology. Specifically, based on comparative bacular morphology, I suggest the borophagines likely had long copulatory durations and spontaneous ovulation, based on the size and simple distal tip of their bacula, respectively. It is possible that with the description of more bacula and further quantitative analysis more robust inferences can be made. The study of reproductive biology in extinct species is challenging and depends on well-established relationships between morphology and behavior or physiology. Nevertheless, further inferences for extinct species could improve our understanding of the selective pressures and consequent evolutionary dynamics of reproductive strategies changing through time. In the long term, it might be possible to better distinguish the role of reproductive function from "phylogenetic inertia" in determining the morphology of the baculum.

Chapter 3

Evolutionary morphology of extant and extinct canid bacula

3.1 Introduction

The genitalia of males evolves rapidly and divergently in many animal groups (Eberhard, 1985), with the result that closely related species may differ only with respect to the morphology of the genitalia. Explanations for this pattern include mechanisms of post-copulatory sexual selection (Hosken & Stockley, 2004; Simmons, 2014; Brennan & Prum, 2015), such as cryptic female choice (Eberhard, 1985, 1996), sperm competition (Parker, 1970), and sexual conflict (Arnqvist & Rowe, 2005) as the drivers of morphological differentiation of animal genitalia. However, it is often challenging to establish a historic record of the evolution of animal genitalia because this structure is generally composed of soft tissue with very little potential for fossilization, which also hinders the ability to compare extant and extinct forms. In this regard, the baculum (*os penis* or *os priapi*) may offer unique insights into the evolution of animal genitalia (*e.g.*, Abella *et al.*, 2013, Chapter 2). This bone is located at the distal end of the penis in species in seven orders of mammals (Stockley, 2012; Schultz *et al.*, 2016b), and because it is a calcified structure it fossilizes much more easily than soft tissues that normally constitute genitalia.

Similar to male genital structures of many other animal groups (Eberhard, 1985), the baculum shows exceptional morphological differentiation among species (Pocock, 1918; Chaine, 1926; Burt, 1960). Since the early 1900s, this variation has been used to help inform the systematics of some mammalian groups. For example, Pocock (1923) used the baculum (together with the glans penis) to define subfamilies of squirrels. Similarly, bacular morphology was used to infer relationships among species of *Mustela* (the genus of weasels and relatives Abramov, 2000), sea lions (Morejohn, 1975), chipmunks (White, 1953), pigmy mice (Packard, 1960) and kangaroo rats (Best & Schnell, 1974). The baculum can also be very useful for taxonomic identification down to the levels of genera and species. For example, Baryshnikov *et al.* (2003) observes that "the baculum as a whole is diagnostic of most genera"

of mustelids.

Despite the long recognition that the baculum is informative for systematics, only recently have hypotheses for its function(s) started to be investigated in comparative studies that aim to understand the mechanisms driving the evolution of the baculum. There is growing evidence that the baculum is subject to post-copulatory sexual selection, despite earlier ideas that its variability might be driven by pleiotropy and drift (see discussion in Patterson & Thaeler, 1982). For example, in the Order Carnivora, induced ovulators show higher complexity at the tip of the baculum than species in which ovulation is spontaneous (Brassey *et al.*, 2020). Further, bacular complexity varies across mating systems, given that species with multiple breeding females that live in groups have less complex bacula than socially monogamous and solitary species (Brassey *et al.*, 2020). Also in carnivorans, the baculum may play a role in sperm competition given that its length is correlated with testes mass (Ramm, 2007; Brassey *et al.*, 2020), which is a good proxy for sperm competition in mammals (Lüpold *et al.*, 2020). Furthermore, the length of the baculum has been found to correlate with the duration of copulation (Dixson, 1987a, 1995; Brindle & Opie, 2016), although this relationship may be weak (Larivière & Ferguson, 2002; Brassey *et al.*, 2018, 2020).

The baculum of canids is very distinctive and easy to recognize at the family level due to a combination of features, such as its deep ventral groove, a dorsal crest, a simple distal end, and the presence of soft tissue attachment scars on the proximal end. The ventral groove and dorsal crest help make the baculum of canids robust (Brassey *et al.*, 2018) which correlates strongly with prolonged copulations, and has been interpreted as being the result of post-copulatory sexual selection (Brassey *et al.*, 2018). Despite these distinctive features, few studies have examined quantitatively the morphological variation of canid bacula. The first such studies (Pohl, 1911; Chaine, 1926; Didier, 1946) described the bacula of 10 species based on a few specimens each, mostly from Europe and Africa. Hildebrand (1951) compared the baculum of 10 species, mostly from the Americas but with some overlap with previous work (the gray wolf and red fox, but from the Americas not Europe). Burt (1960) included more specimens in his description of the bacula of five North American canid species. More recently, Brassey *et al.* (2018, 2020) included one representative specimen of 16 species of canid, among a larger analysis of the main lineages of Carnivora. These authors were interested in the relationship of 3D baculum shape with reproductive traits. There are also accounts of the variation of the baculum within single species of canids, the domestic dog, grey wolf, and red fox (*e.g.* Sharir *et al.*, 2011; Čanády, 2013; Čanády & Čomor, 2015) that show high levels of intraspecific variation. However, a more complete quantification of the intraspecific variation of the canid baculum and how morphological differentiation has evolved among species is currently missing from the literature.

Here, I compare the morphology of the bacula of 26 extant species of canids (out of the 35-40 named species), as well as 4 extinct species. My goals were to: (1) determine the degree to which species and genera can be differentiated based on bacular size and shape; (2) compare the morphologies of extant and extinct taxa; and, (3) determine whether ancestral state reconstruction based on living taxa can be used to predict the morphologies of extinct ones. To investigate these goals, I used elliptical Fourier analysis to build a 2D morphospace based

on the lateral view of the baculum. The average position of species on the morphospace was used in phylogenetic comparative methods to infer ancestral state as well as the correlation with duration of copulation. Canids provide one of the few opportunities to conduct this analysis, as the group has the highest number of known fossil bacula, representing seven extinct species (Wang, 1994; Hartstone-Rose *et al.*, 2015, Chapter 2). However, only four of those species have fossil bacula that are complete and undistorted that can have their shape compared with extant ones and were included in this study.

3.2 Materials and Methods

Museum abbreviations

MVZ, Museum of Vertebrate Zoology, University of California, Berkeley, California; UCMP, University of California Museum of Paleontology, University of California, Berkeley, California; FMNH, Field Museum of Natural History, Chicago, Illinois; AMNH, American Museum of Natural History, New York, New York; F:AM, Frick Collection, American Museum of Natural History, New York, New York; USNM, National Museum of Natural History, Smithsonian Institution, Washington, D.C.; MCZ, Museum of Comparative Zoology, Harvard University, Cambridge, Massachusetts. For museums containing both modern and fossil material, I have appended VP or M to the appropriate abbreviation to indicate the vertebrate paleontology versus mammalogy divisions in those collections.

Specimens examined

For extant species I sampled 128 adult specimens from 26 out of the 35-40 recognized canine species, representing 11 out of the 12 recognized extant genera (*Cuon* was the only genus not sampled). The size and shape of the baculum typically changes with ontogeny (*e.g.*, Wright, 1947; Elder, 1951; Friley, 1949). In canids, both the proximal and distal ends change with age (Hildebrand, 1951). For example, tissue attachment scars on the proximal end are not present or are difficult to observe in newborns to subadult individuals. Further, while the distal end is porous in young individuals, it is smooth in adults (Hildebrand, 1951). Accordingly, I only took measurements from the bacula of adults. Whenever possible, I assessed skeletal features, such as the presence of open symphyses on long bones or unerupted teeth to distinguish juveniles from adults. Table A.1 provides a list of all specimens included in my analyses.

For all specimens, analyses of bacular shape were based on photographs taken of museum specimens, augmented by published images. For fossil materials, I sampled one specimen of the dire wolf (*Aenocyon dirus*) from the UCMP, which is a largely complete baculum, at least in left lateral view. I also used four images of dire wolf bacula from Hartstone-Rose *et al.* (2015, ontogenetic stage 2.5 and higher in their Figure 3). For *H. gregarius*, I used the outline of the baculum from a drawing in Wang (1994) that is a composite of two specimens,

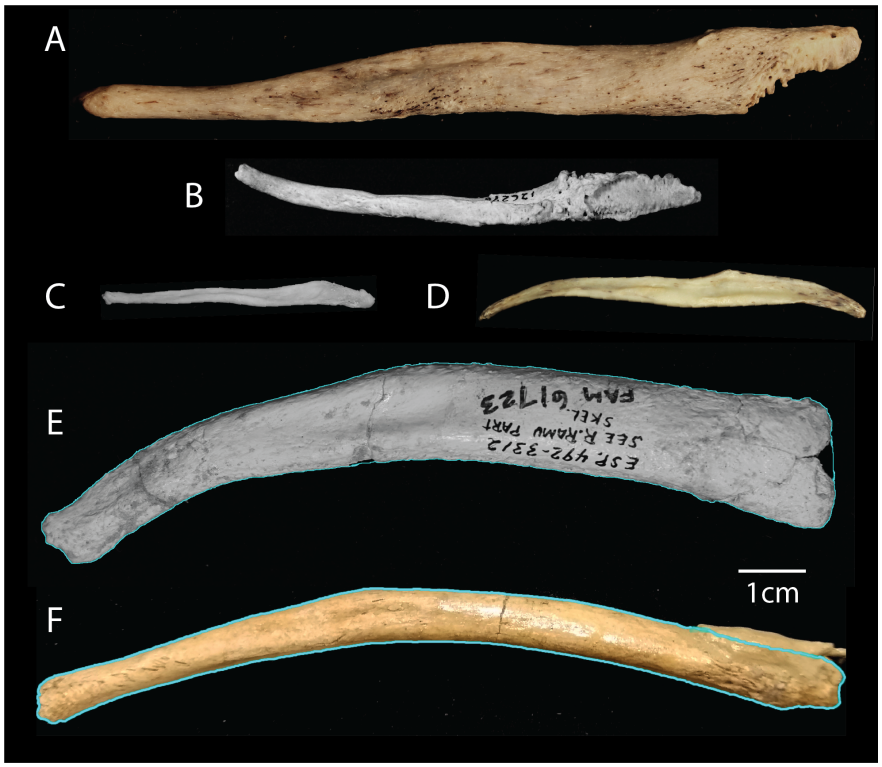

Figure 3.1: Examples of canid bacula in left lateral view with the distal end at the left. Blue borders (E,F) represent the inferred complete outline for a broken and a mounted specimen. A) Gray wolf (*C. lupus*), B) Bush dog (*S. venaticus*), C) Kit fox (*V. macrotica*), D) Gray fox (*U. cinereoargenteus*), E) *Aelurodon ferox*, F) *Aelurodon stirtoni*.

primarily MCZ 3667 but with the proximal end of FMNH-VP 12224. For *Aelurodon stirtoni* I used photographs of USNM-VP 215320 sent to me, and for *Aelurodon ferox* I photographed F:AM 61723 (Chapter 2).

The baculum of each specimen was photographed in left lateral view (Figure 3.1). For a few specimens this view was precluded (*e.g.*, obstructed by museum label or soft tissue still present); for these specimens, the right side was photographed. The image was then mirrored for comparison with the other specimens. This process assumes bilateral symmetry of the baculum. Although I have occasionally observed slight asymmetries in canid bacula, I have never seen consistent patterns of significant asymmetry, such as those reported in the Mustelidae (Long & Frank, 1968; Baryshnikov *et al.*, 2003).

Analysis was based on masks of the original images. Outlines were created by using Photoshop (Adobe Photoshop CC 2019 for Mac) to convert the images into black silhouettes on white backgrounds. The images of two of the fossil bacula required additional editing. The baculum of *Aelurodon stirtoni* is part of a skeleton on public display. To generate its outline I digitally removed the mount that obscures the dorsal portion of its proximal end

(Figure 3.1). The baculum of *Aelurodon ferox* is slightly broken at the proximal end; I completed the outline for this specimen by following the curvature of the unbroken portions of the bone (see Figure 3.1). As a control, I also conducted analyses using the broken outline of the bone, which only had a minor effect on its position in the morphospace (data not shown).

Morphometric analyses

To quantitatively describe the outlines of the canid bacula I conducted elliptical Fourier analyses, as implemented in the R package 'Momocs' (Bonhomme *et al.*, 2014). Elliptic Fourier analysis describes outlines with equations that are composed of hierarchical harmonics (sets of 4 coefficients). These coefficients can then be used to quantitatively compare outlines. Two landmarks were defined for every specimen: the distal and proximal ends, which as extremal points are type III landmarks (Bookstein, 1992). The point on the outline chosen to begin the elliptical Fourier analysis affects the outcome of the analysis (Crampton, 1995), so I used a consistent landmark, the one at the distal end, as the beginning point for all outlines. Outlines were rotated as necessary to align the two landmarks horizontally. Two separate analyses were performed, one with and one without size. For the former, I calculated elliptical Fourier coefficients (function 'efourier') based on images that were scaled to the measured length of the baculum. For the second analysis of shape alone, I calculated the Bookstein coordinates (function 'coo_bookstein') which standardize the distance between the two landmarks (set to a value of 1). I refer to the first as the analysis of *form*, which includes size and shape, and the second as the analysis of *shape* alone. In both cases I kept 11 harmonics, each of which consists of 4 coefficients, to describe the outlines, which explained over 99% of the variance in the form and shape of the bacula analyzed. Next, I performed a principal component analysis (PCA) on the 44 harmonic coefficients, which were visualized using the function 'PCcontrib' in Momocs.

To determine the degree to which species and genera can be differentiated based on bacular morphology, I used a Linear Discriminant Analysis (LDA) on PCA scores for both form and shape. LDA maximizes the discrimination between pre-defined groups, in this case, species and genera. To assess the discriminatory power of the analysis I used the percentage of specimens correctly assigned to their taxon in a leave-one-out cross-validation test, as included in the LDA function in the Momocs package. Given that the percentage of specimens correctly assigned to their taxon varies depending on the number of PCs retained in the LDA, I repeated the LDA using from 2 to 30 PC axes; below I report only the cross-validation test results for the analysis with the highest percentage of specimens correctly predicted to species. Note that the leave-one-out test could not be applied to the 7 species represented by only one specimen (*H. gregarius*, *A. ferox*, *A. stirtoni*, *V. chama*, *L. adusta*, *C. rufus*, and *U. littoralis*). I also performed an LDA at the genus level. For this analysis, *Hesperocyon* was the only genus excluded due to being represented by only one specimen.

Phylogenetic Comparative Analysis

The position of the fossil bacula in the morphospace relative to extant species shows that bacula shapes for stem canids differ from those for extant canines (see Results). To address if this difference is expected given the branch lengths separating stem and extant taxa, I performed ancestral state reconstruction (see below). I use these reconstructions as a first approximation for understanding the effect of including fossils in analyses of the evolution of bacular shape in canids. For this purpose, I focus on the comparison between the inferred ancestral states of the crown group of the subfamily Caninae versus the ancestral state of the entire family Canidae with the stem fossils included, paying particular attention to the position of stem fossils in the distribution of possible ancestral states.

Species-level data

Prior to ancestral state reconstruction, I aggregated the specimen-level data on bacular shape to the species level. This was done by calculating the average of the harmonic coefficients for each species, using the function 'MSHAPE' (in package 'Momocs', in R). I then performed a new PCA of baculum shape based on these species averages, and I used the PCA scores of each species for the ancestral state reconstruction.

Phylogeny used

Several phylogenies exist for the family Canidae (*e.g.,* Wayne *et al.*, 1997; Perini *et al.*, 2010; Zrzavý *et al.*, 2018; Porto *et al.*, 2019; Lamarca & Schrago, 2020). Here I used the same phylogeny as Machado (2020) because it is the most recent phylogeny reconstructed from molecular and morphological data with information from fossils. In this phylogeny, the topology for the extant species is from Zrzavý *et al.* (2018), which was constructed using total evidence maximum parsimony. The tree was time-calibrated using the fossil record by Machado (2020).

I added the four extinct species for which complete bacula are available (see above) to the phylogeny, following Perri *et al.* (2021) for the position of the dire wolf and Slater (2015) for the positions of the other three species. Ancient DNA recovers dire wolves as sister to all extant members of the "wolf-like" group Canina (*Canis*, *Lupullela*, *Cuon* and *Lycaon* - Perri *et al.*, 2021). Using these phylogenetic relationships, I grafted the branch for dire wolf onto the tree as stem-group Canina at the following three positions: (1) at the very base (close to the divergence to South American canids, the Cerdocyonina); (2) in the middle of the branch; and, (3) at the very top of the branch (right before the split of crown Canina). Collectively, these placements cover all possible lengths for the branch leading to the dire wolf.

The phylogenetic relationship among the Caninae, Hesperocyoninae, and Borophaginae is unresolved. Slater (2015) recovered a polytomy for these three subfamilies at the base of the canid phylogeny. I analyzed each of the three possible resolutions to this polytomy (Figure B.1). Each resolution contained two nodes, an older and a younger node (Figure

B.1). I used two sets of node ages for each topology. Based on the 95% credibility interval for the posterior age distributions provided by Slater (2015) I (1) used the maximum values of the confidence interval for the first and second nodes at 42.15 and 41.5Ma, respectively, and then (2) used the youngest values of the confidence intervals to define node ages at 40.15 and 37.65Ma. The analyses requiring these age estimates (the ancestral character state reconstructions) were revealed to be insensitive to these dating uncertainties, and thus I only report the results for the phylogeny with the Hesperocyoninae as the basal subfamily in the main text.

I established the branch lengths for the extinct species using the range of divergence times described above and the age of their last occurrence in the fossil record. Last occurrence dates were the top of the Whitneyan (30.8Ma) for *H. gregarious*, the top of the Clarendonian (10.5Ma) for *A. ferox*, and the top of the Late Barstovian (12.5Ma) for *A. stirtonii*. Because the first occurrences of both species of *Aelurodon* are in the Late Barstovian, I used its base for the divergence time between the two species; this is similar to the consensus phylogeny in Slater (2015). While the assignment of branch lengths in phylogenies with fossils is complicated, Bapst (2014) demonstrated that results of comparative methods based on phylogenies that include extant species are less sensitive to these uncertainties (but see Bapst, 2014, for a more complete discussion of this issue). Furthermore, this is a conservative approach for the ancestral state reconstruction given that by using last occurrences I have maximized the amount of time during which bacular morphology may have evolved, thereby over-estimated the variance in the ancestral character state.

Ancestral State Reconstruction of Shape

I used the position in the new PCA of the shape for each species to perform ancestral state reconstructions (ASR) using the function 'fastAnc' in the package 'phytools' (Revell, 2012). I analyzed each of the first 8 PCs separately, which together accounted for 98% of the variance in shape in the total sample. The ancestral state reconstruction is based on the following three assumptions: (1) evolutionary change occurred under Brownian Motion (BM), (2) evolutionary change on each PC is independent of changes on the other PCs, and (3) each PC has one constant value for the rate of evolution (σ^2_{bm}, the parameter of BM). Although I did not test these assumptions, they serve as a null hypothesis for the evolution of bacular shape.

Preliminary inspection of the results of these analyses suggested that the fossils drive the inferred ancestral state at the base of the canid phylogeny on PC1 and PC2, leading the total group ASR to lie outside the range of morphologies observed for extant species (see Results). To evaluate this possibility I examined the probability of inferring the total group ancestral state given a rate of evolution calculated only from extant species and given the estimated time elapsed from the base of the Canidae to the base of the crown group Caninae (29.75 M.y.). To determine if the morphology of the inferred ancestral baculum of canids would lie within the range of predicted morphologies if only data from the extant species were analyzed, I employed the following steps:

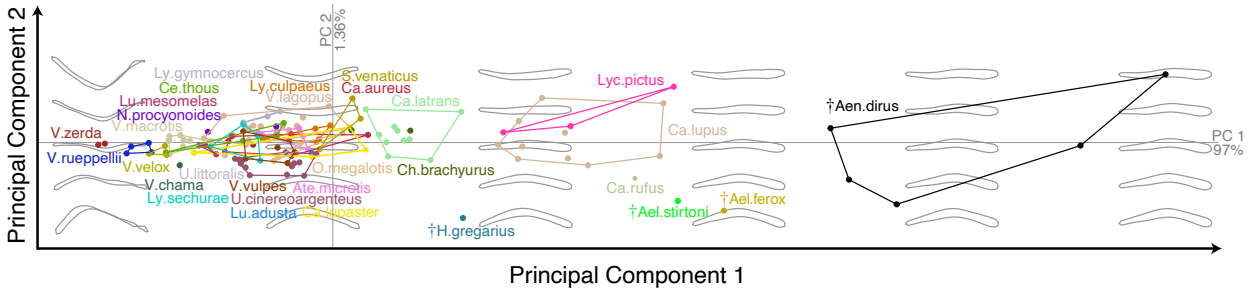

Figure 3.2: Morphospace for the form (shape and size) of the baculum of canids. PC1 captures 97% of the variation and largely represents size, with the largest bacula at the right. Note that there is a cluster of mid-sized species with an extensive overlap in the morphospace. PC2 captures just 1.36% of variance. Outlines of bacula on the background are the predicted shapes given the PC1 and PC2 scores. The distal end is at the left, the proximal end at the right. †Extinct species.

- For extant species only, I calculated the mean and variance (m_ℓ,σ^2_ℓ) of the inferred ancestral state on PC1 and PC2 (each axis analyzed separately), using the function 'fastAnc' (package 'phytools');
- I calculated the rate of evolution (σ^2_{bm}) under Brownian motion, using the function 'fitContinuous' (package 'geiger', Pennell *et al.*, 2014), with the evolving trait being the species' positions on PC1 and PC2.
- I inferred the distribution of ancestral states for the time of the oldest divergence event in the canid phylogeny, assuming the same constant rate of evolution from the previous step (*i.e.* I project the range of possible ancestral states to 29.75 M.y. before the crown age of canines). Given the assumption of Brownian motion, this is a normal distribution with parameters $\mathcal{N}(m_\ell, \sigma^2_\ell + 29.75\sigma^2_{bm})$.
- I determined the overlap of the normal distribution from the previous step with the 50% and 95% confidence intervals for the ancestral state reconstructions that included fossils.

3.3 Results

Morphospace of form and shape

The first component of the PCA for form accounts for 97% of the variance observed (Figure 3.2). This axis corresponds primarily to the size of the baculum (distance between the distal and proximal ends, Figure 3.2) with a strong positive correlation between baculum length and the PC1 score $r = 0.99$ ($p < 10^{-16}$). Visual inspection of the PCA plot for this analysis suggests that PC1 enables the best differentiation among species (confirmed with

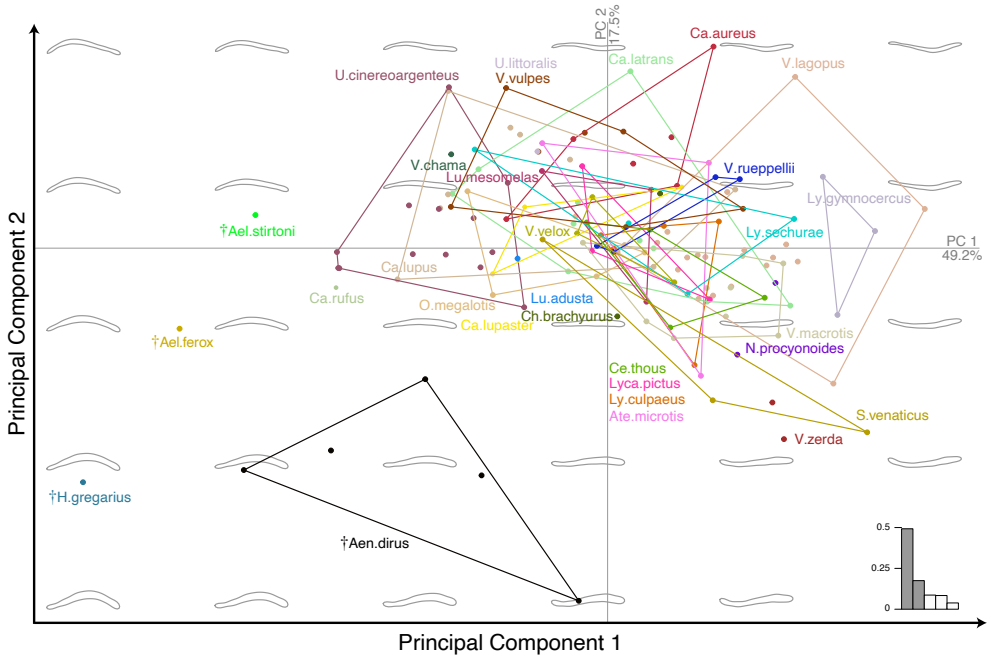

Figure 3.3: Morphospace for the shape of the baculum of canids. PC1 describes 49.2% of the variation of shape and largely describes the primary curvature of the baculum, with the arched bacula at the left and upcurved bacula at the right. PC2 captures 17.5% of variance of shape and describes largely secondary curvature and aspect ratio of bacula. Outlines of bacula on the background are the predicted shapes given the PC1 and PC2 scores. The distal end is at the left, the proximal end at the right. †Extinct species.

LDA, see below). Although most specimens are concentrated in the same region of PC1 and PC2, large-sized species can generally be differentiated from the main cluster and from each other. For example, all dire wolf specimens stand out on PC1, being much larger than the bacula of other canids. Several large species occupy unique portions of the morphospace, for example, both species of *Aelurodon*, wolves (*C. lupus* and *C. rufus*), African hunting dogs (*Lycaon pictus*) and coyotes (*C. latrans*). The area of the morphospace with the highest density of specimens shows an extensive overlap of species, especially on PC1. This cluster is composed primarily of intermediate sized species, such as the culpeo (*Lycalopex culpaeus* – ∼8kg), red fox (*Vulpes vulpes* – ∼6.3kg) and golden jackal (*Canis aureus* – ∼9.55kg; data on body mass from Sillero-Zubiri *et al.*, 2004); these taxa cannot be visually differentiated from each other in the morphospace. At the smaller end of PC1 there are fewer species and it is easier to differentiate species (*e.g.*, *Vulpes zerda*, *V. rueppellii*, and *V. velox*) in this region of the morphospace.

Analyses of baculum shape reveal that PC1 largely describes the primary curvature of the baculum and accounts for 49.2% of the total variation in shape (Fig. 3.3). PC2 captures a

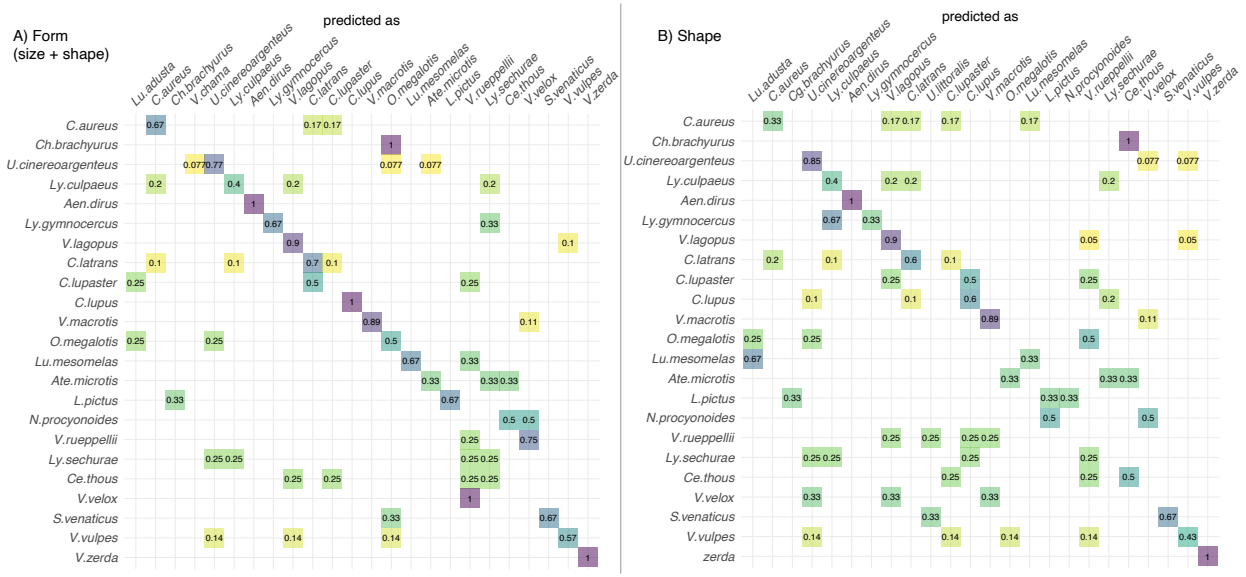

Figure 3.4: Species-level percent of specimens correctly predicted from the LDA leave-one-out cross-validation test. Table (A) is for baculum form, and (B) is for baculum shape.

combination of secondary curvature and the baculum aspect ratio (Fig. B.2), accounting for 17.3% of the total variation in shape. In some species all specimens have a curved baculum forming an arch such that the tip points ventrally (*e.g.*, gray fox *U. cinereoargenteus*, n = 13). In other species, the baculum is upcurved and the tip points dorsally (*e.g.*, arctic fox, *Vulpes lagopus*, n = 20), or it may be arched or upcurved (*e.g.,* coyote, *C. latrans*, n = 10). The most striking pattern is that the stem fossils, those of the Hesperocyoninae and Borophaginae, stand out on PC1 of shape (Fig. 3.3), reflecting the observation that *H. gregarius*, *Aelurodon ferox* and *Aelurodon stirtoni* have bacula that are more strongly arched than the bacula of the Caninae. *H. gregarius* and dire wolves are also distinct from all other canids in PC2 (Fig. 3.3). The distinctiveness of these two species is due to their bacula having a proportionally taller (dorso-ventral) height, with the peak of the dorsal ridge occurring closer to the proximal end rather than the middle of the shaft, as is seen in other taxa. Then, higher PCs (PC3, PC4, etc.) account for variation in the relative thickness along the baculum and curvatures restricted to the dorsal or ventral sides (Figure B.2).

While the fossil specimens stand out in the PCA for shape, there is much overlap in the morphospace among extant species, making it difficult to differentiate them based on baculum structure. Nevertheless, a slight difference in morphospace occupancy is evident between the sister clades Cerdocyonina and Canina, with the former tending to have more dorsally curved bacula (see the right end of PC1 of Fig. 3.3), while the latter have mostly straight to slightly arched bacula. This pattern is easier to observe from the average shapes of species (see below). In general, however, there is considerable overlap among extant species.

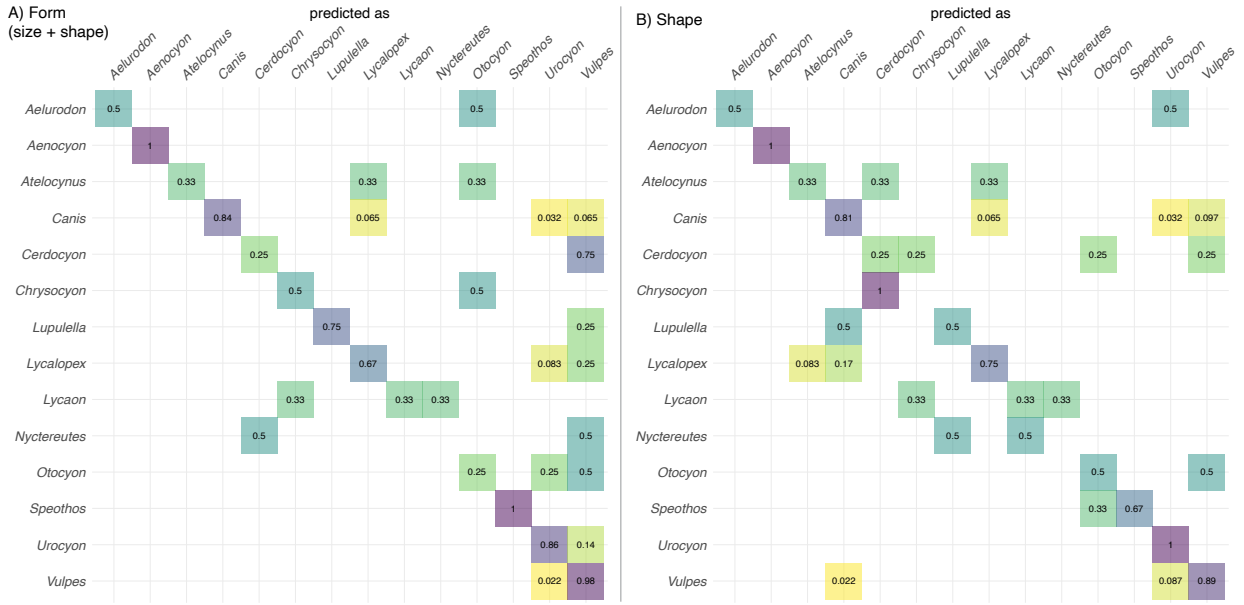

Figure 3.5: Genus-level percent of specimens correctly predicted from an LDA leave-one-out cross-validation test. Table (A) is for baculum form, and (B) is for baculum shape.

LDA

The LDA revealed that different species of the Canidae are not easily differentiated based on the lateral profile of the baculum. Consistent with visual inspection of PCA figures (Figs. 3.2 and 3.3), size allows for more differentiation among species than shape alone. When size is included, 66.7% of the specimens are correctly associated with their conspecifics in the leave-one-out cross-validation test when 19 PC axes retained (Fig. B.3A). This drops to 54.3% correct assignment when size is excluded (14 PCs retained – Fig. B.3B). Only the dire wolf (n = 5) and the Fennec's fox (*Vulpes zerda*, n = 2) had all specimens correctly predicted in both LDAs (form and shape – Figure 3.4). Other species for which most specimens can be correctly predicted are the gray fox (77% form and 85% shape) and the arctic fox (90% in both form and shape).

At the generic level, the overall correct assignment of specimens to genus was 80% for form and 77% for shape (with 18 and 20 PCs retained respectively). For baculum form, most incorrect predictions were in the direction of incorrectly predicting the specimen to be in the genus *Vulpes*. For baculum shape, incorrectly predicted specimens are associated to many different genera. The genera that were best predicted with regard to both, form and shape were *Aenocyon*, *Canis*, *Lycalopex*, *Speothos*, *Urocyon* and *Vulpes*.

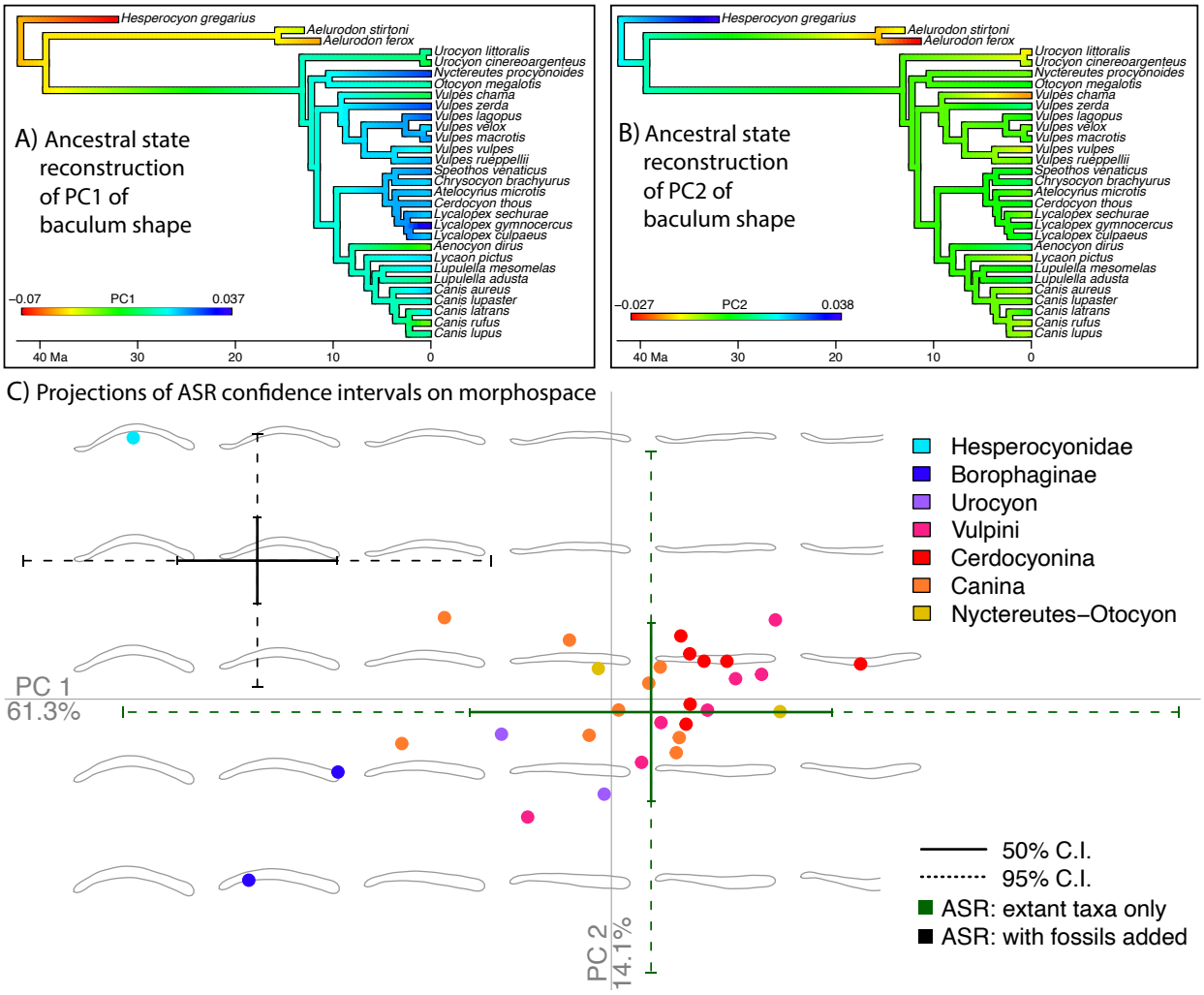

Figure 3.6: Ancestral state reconstruction (ASR) for the vales of the PC scores for baculum shape. The calculations were done with the Hesperocyoninae as basal, but the results are insensitive to the alternative topologies (Fig. B.4). A) PC1 and B) PC2. C) Baculum shape morphospace where each point represents a species colored by clade (see legend). The inferred range of the ancestral character states with the fossils included is indicated by the black lines, where dashed lines are the 95% and continuous lines the 50% confidence intervals. The green lines show 95% and 50% confidence intervals from the ancestral state recovered with the data from the extant species only, projected back to 42.25Ma.

Ancestral state reconstruction

Ancestral state reconstruction for PC1 scores from the shape analysis (which corresponds primarily to the curvature of the baculum) revealed a very different average between the node at the base of the crown group versus the node for the total group (total=crown+stem, Fig 3.6A – PC1 total group = -0.052085, 95%C.I. -0.086607 to -0.017563; crown-group = -0.000116, 95%C.I. -0.021153 to 0.020920). This result was robust to the variations in the phylogeny reflecting uncertainties in the evolutionary relationship among some taxa and thus I present results for just one tree (see supplementary Fig. B.4 for the full set of values). The reconstructed values for PC1 suggest that the ancestral baculum for canids was strongly arched, a morphology that is quite different from the majority of extant species. Only two canines (dire wolf, $n = 5$, and the red wolf *C. rufus*, $n = 1$) are sufficiently arched to lie within the 95% confidence interval for the reconstructed ancestral values for PC1 for canids. Similarly, the estimated ancestral values for PC2 for the total group are different from those for the crown group (Fig 3.6A – PC2 total group = 0.020377, 95%C.I. 0.001677 to 0.039077; average PC2 state of crown group = 0.000178, 95%C.I. -0.011217 to 0.011574). The short temporal distance between *H. gregarius* and the base of the tree suggests that this species may have a stronger effect on the reconstruction for PC2 than the other stem fossils (*e.g.*, *Aelurodon*). *H. gregarius* is a morphological outlier on PC2 and this may have contributed to the finding that no species fall within the 50% confidence interval for this ancestral state reconstruction. In contrast, the reconstructions for PC3 through PC8 did not reveal differences between the inferred ancestral character states for the crown group and total group nodes; this result is robust to the tree topology used (Fig. B.4).

Using only extant species to project the ancestral state reconstruction of baculum structure generated different mean values from those obtained when fossil specimens were included (see the intersection of green lines *vs.* black lines in Fig. 3.6C). This is perhaps not surprising given that the fossil specimens of stem group occupy a different area of the morphospace than those from extant species. However, the long time interval between the stem subfamilies and the crown group of the Caninae leads to a very large uncertainty around the average values, providing a 95% confidence interval that encompasses the ancestral state reconstruction with fossils.

Despite the wide range of possible ancestral character states inferred for extant taxa, the inferred range of ancestral morphologies when fossils are included displays little overlap with the results of the extant-only inference. For example, for PC1, using only extant species results in a 7.22% chance of inferring that the ancestral baculum was at least as arched as the average inferred ancestral state when fossils are included. Furthermore, only 8.38% of the inferred distribution along PC1 for extant species overlaps with the 50% C.I. for ancestral states inferred with fossils; this probability increases to a 26.78% chance of overlap when the 95% C.I. is considered. There is a greater overlap between the inferred ancestral character states with and without fossils for PC2, with 13.79% and 40.92% overlap with the 50% and 95% C.I.s, respectively.

3.4 Discussion

Although the bacula of the Canidae are distinctive at the family level, they are not strongly diagnostic at the species or genus levels. Nevertheless, a few distinctive morphologies are observed, including the extremes of baculum size, and the shape of the bacula of the extinct species included in this study. Below I discuss the challenges of differentiating the bacula of canid species and genera, after which I consider the distinctiveness of the fossil taxa examined.

Linear discriminant analysis (LDA) provided limited power to identify bacula to species based on the morphology of its conspecifics. The predictive power of these analyses was greater when both shape and size were considered, compared to analyses on shape alone. These analyses were better able to identify bacula to genera, with this ability again being greater when both shape and size were considered. However, including size for LDA increased the success rate of prediction very little, in comparison to the success rate of shape alone (from 54.3 to 66.7% for species, and from 77 to 80% for genera), suggesting that most of the information comes from shape. Thus, use of elliptical Fourier analysis adds substantially to the ability to distinguish among the bacula of canids, especially considering the lack of distinct reference points for placing landmarks that allow few standardized measurements that can be made to compare specimens.

Given the extensive species overlap in the baculum morphospace, it is not too surprising that the LDA was unable to reliably assign specimens to species and genera. Incorrectly assigned specimens typically belonged to species or genera for which: (1) sample sizes were small (often just two specimens), (2) specimens were well dispersed in the morphospace, and, (3) all specimens from other taxon fell between members of the misidentified taxon in the morphospace. For example, the maned wolf (*Chrysocyon brachyurus*) and the raccoon dog (*Nyctereutes procyonoides*) are each represented by two well-dispersed specimens that bracket other species in the morphospace (Fig. 3.3). In both cases, the leave-one test typically assigns one individual to the taxon that lies between the specimens of the focal taxon (Fig. 3.4). Larger sample sizes should increase the density of points between the few samples available and therefore reduce the number of misdiagnosed specimens by analyses such as LDA.

Furthermore, the results presented here are based on the analysis of 2D lateral views and it seems likely that additional information on the morphology of each specimen would improve the ability to diagnose species. For example, the baculum of the bush dog, *Speothos venaticus*, has attachment scars on the proximal end that are much more strongly developed than in other canids (*e.g.*, see Fig. 3.1B), making the baculum of this species straightforward to identify by visual inspection. However, this feature is largely invisible in the lateral 2D outlines and thus does not contribute to the morphospace (the scars only lead to minor projections seen in the outlines). Thus, it is likely that 3D data would have increased diagnostic power.

The elliptical Fourier analyses reported here are based on the largest sample size of canid bacula studied to date. The results of this study are consistent with previous work which

noted the "fairly uniform" (Burt, 1960) morphology of the bacula of canids. The conserved morphology of canid bacula at the family level contrasts with other closely related families within the suborder Caniformia. Most strikingly is the variation of bacula observed in the family Mustelidae, members of which have bacula that are easily distinguished, especially at the distal tip which may bifurcate (Sable, *Martes zibellina*), be diamond-shaped and twisted (American badger, *Taxidea taxus*), or have additional projections (Yellow-throated Marten, *Martes flavigula*, Baryshnikov *et al.*, 2003). This difference between these two families is potentially associated with other differences in their reproductive strategy that has been shown to correlate with baculum morphology (Brassey *et al.*, 2020, such as mating system and ovulation strategy). For example, higher complexity of the distal tip has been associated with induced ovulation (Brassey *et al.*, 2020), which is more common in mustelids than in canids.

The most distinctive species in the morphospace is the dire wolf, both in size (form) and shape (Figures 3.2 and 3.3). If bacula structure plays a role in reproductive isolation, then this distinctiveness may have represented a barrier to hybridization with close relatives, such as members of its sister group, the sub-tribe Canina (the "wolf-like" canids). This hypothesis is supported by data from the dire wolf genome, which provides no evidence of introgression between the dire wolf and its closely related, sympatric species, including the gray wolf and the coyote (Perri *et al.*, 2021). This is remarkable given the multiple examples of gene flow among members of Canina (Koepfli *et al.*, 2015; VonHoldt *et al.*, 2016; Gopalakrishnan *et al.*, 2018), one example is the gray wolf and the coyote, which have very similar bacula (Figure 3.3). Although there is evidence of hybridization between species that have a baculum different from each other (*e.g.*, in chipmunks, Good *et al.*, 2003), the differences in size and shape of the baculum of dire wolves in comparison to other closely related canids suggests that, in this case, bacular structure could be involved in reproductive isolation.

The bacula belonging to the stem groups Hesperocyoninae and Borophaginae are also distinctive, being strongly arched compared to the mostly straight bacula of extant canids. An arched shape is also seen in fossil bacula from three borophagine species not examined here because they are only partially preserved (Chapter 2), but they add support to the hypothesis that this is a general feature of the borophagines.

The ancestral state reconstruction of PC1, which captures the curvature of the bacula (Figure 3.6), was strongly driven by the archness of the bacula of the stem fossils. Consequently, the inferred ancestral morphology was more arched than any extant species, with only two species of the Caninae within the 95%C.I. of the distribution of the ancestral state reconstruction (the dire wolf and *Canis rufus*). This suggests that the morphology of the stem fossils is arched to a level that is not expected given the morphology of extant canids.

However, it is important to interpret the results of ancestral state reconstructions carefully, as these kinds of analyses are just the most simple statistical model that can be used to infer a distribution of morphologies given the observed variation in the taxa sampled and the branch lengths (*i.e.* total time during which this variation evolved). Further, the model used for ancestral state reconstructions (Brownian motion) assumes that lineages evolved random changes through time, and that generates the expectation that differences in mor-

phology among lineages increase with time. Given these assumptions of the model, I do not claim that the results of these analyses predict the actual ancestral morphology of the baculum of canids, but they represent an informed hypothesis. Using extant species alone to hypothesize ancestral states, results in a very low probability of recovering ancestral morphologies as arched as inferred with the stem fossils (Figure 3.6). In other words, given the mostly straight morphology of the baculum of extant species and the rate of accumulation of morphological differences among them, the long divergence time between stem and crown groups is not enough to predict (with high probability) the curvature of the bacula observed in stem fossils, neither the ancestral state inferred when the fossils were included. These results highlight the importance of adding fossils when inferring ancestral morphologies (Slater *et al.*, 2012).

The discordance between ancestral morphologies inferred with and without fossils offers information about the likely mode of evolution between the crown group taxa and the base of the canid clade. The failure of the Brownian motion model to reliably predict the ancestral morphology when only extant taxa are included suggests a directional mode of evolution for the baculum of canids. Alternatively, a change in the rate of Brownian motion may have occurred somewhere within the lineage leading to the living canids.

The hypothesis of directional change playing an important role in the evolution of the baculum makes sense in light of the reproductive strategies of modern canids. In particular, all modern canids have a copulatory tie (Kleiman, 1968; Asa & Valdespino, 1998) that frequently leads to long copulatory durations. Brassey *et al.* (2018) showed that longer copulatory durations are strongly associated with more robust bacula across all carnivorans. Further, bacula that are dorsally curved are more robust to the type of dorso-ventral bending forces investigated by Brassey *et al.* (2018). This suggests that the arched bacula of the stem fossils are less robust than those of modern canids, which could help explain the selective forces driving the directional evolution of the baculum, but this remains to be tested in future investigations.

Chapter 4

Evolutionary allometry of the canid baculum

4.1 Introduction

The baculum (penis bone, *os penis*, *os priapi*) has a remarkable range of morphologies (Burt, 1960; Stockley, 2012), with the bacula in some species having spines, while others have hooks, holes, split-ends, or grooves. There are also large differences in size, with some bacula being over half-a-meter long (*e.g.*, walruses, Fay, 1982) and others just a few millimeters in length (*e.g.*, jaguar, mice, and bats Didier, 1949; Csanády *et al.*, 2019; Hosken *et al.*, 2001).

Multiple hypotheses have been generated to explain this morphological variation and function of the baculum (*e.g.*, Long & Frank, 1968; Patterson & Thaeler, 1982; Larivière & Ferguson, 2002; Stockley *et al.*, 2013; Herdina *et al.*, 2015; Brassey *et al.*, 2018, 2020), especially the variation in size (*e.g.*, Dixson, 1987a; Larivière & Ferguson, 2002; Dixson *et al.*, 2004; Kinahan *et al.*, 2008). For example, it has been proposed that baculum length is associated with prolonged intromission duration (Dixson, 1987a, 1995; Dixson *et al.*, 2004; Brindle & Opie, 2016, but see Larivière & Ferguson 2002; Brassey *et al.* 2018) and larger testis mass (Hosken *et al.*, 2001; Ramm, 2007; Brassey *et al.*, 2020), suggesting that baculum length plays a role in post-copulatory sexual selection.

Typically, analyses of baculum length treat body size as a covariate intended to normalize differences in body size; only a few studies have analyzed the evolutionary allometry of the baculum for its own sake. In the largest scale study of this nature, Ramm (2007) found a negative allometric slope and low values for the coefficient of determination ($r^2 \approx 0.12$) in an analysis of a wide range of taxa (Rodentia, Chiroptera, Carnivora, and Primates), indicating that a large portion of the among species differences in baculum length is not explained by differences in body mass. This author concluded that "genital size in mammals evolves to a large extent independently of body size". This conclusion is consistent with many studies that used smaller sample sizes (*e.g.*, Hosken *et al.*, 2001, for bats) and a narrower taxonomic scope (within genera or families, *e.g.*, Best & Schnell, 1974; Patterson & Thaeler, 1982;

Patterson, 1983).

Nevertheless, larger values of allometric slopes that seem to deviate from the allometric relationship reported by Ramm (2007) have been recovered in a few studies. For example, Dixson *et al.* (2004) reported a slope near isometry in a combined analysis of rodents, carnivorans, and primates. However, Dixson *et al.* (2004) did not account for phylogenetic auto-correlation in the data, which may bias their slope estimates and highlights the importance of correcting for phylogeny to draw conclusions related to evolutionary allometry. Baryshnikov *et al.* (2003) also found allometric slope values larger than those reported by Ramm (2007) in a study of Caniformia and Mustelidae based on phylogenetic independent contrasts. Although Baryshnikov *et al.* (2003) did not report values for allometric slope in their analysis, their figures indicate slope values between 0.5 and 1. Despite this relationship being significant, it was not strong ($r^2 = 0.36$) after accounting for phylogeny.

Here, I investigate the evolutionary allometry of the baculum within the family Canidae using data from 26 (out of 35–40) extant and four extinct species within this family. Specifically, I examine whether canids follow the overall mammalian trend of negative allometry for the baculum. Few comparisons of proportional baculum size have been undertaken for extinct species, and those that have been made (Wang, 1994; Hartstone-Rose *et al.*, 2015) have relied directly on baculum:body-size ratios without accounting for changes in proportion that are expected from allometric relations. As a result, in addition to providing novel insights into relationships between baculum and body size in canids, my analyses generate important insights into the relevance of these relationships to extinct members of this carnivoran family.

4.2 Methods

Taxa included

The family Canidae is divided in three subfamilies: the extant Caninae, and the extinct Hesperocyoninae and Borophaginae. Despite the rich fossil record for canids (Wang, 1994; Wang *et al.*, 1999; Tedford *et al.*, 2009), bacula have been described for only seven extinct species (Wang 1994; Dundas 1999; Chapter 2), three of which are known only from incompletely preserved bacula. Among those with complete bacula, the dire wolf (*Aenocyon dirus*) is the only member of the subfamily Caninae to have been characterized (Hartstone-Rose *et al.*, 2015); the baculum for this extinct species is proportionately larger than that of the extant gray wolf. Wang (1994) established that the baculum of *Hesperocyon gregarius*, the only known specimen for the subfamily Hesprocyoninae, is substantially larger than that of other similar-sized canid species, such as the red fox. The size of the borophagine baculum has not previously been compared with that of other species; here I do so for *Aelurodon stirtoni* and *Aelurodon ferox*.

I sampled 128 specimens across the 26 extant species, as well as 8 specimens from four extinct species examined (Table 4.1). Three of the extinct species (*H. gregarius*, *A. ferox*, and

A. stirtoni) are represented by one specimen only. In contrast, five specimens of *Aenocyon dirus* were sampled, four of which were from published images (Hartstone-Rose *et al.*, 2015). Following procedures in Chapter 3, photographs of the baculum in lateral view were used to make the length measurements. Values for baculum length were then $\log_{10}$ transformed and averaged for each species for which multiple specimens were examined (Table 4.1).

For body size, I compiled data on average male body masses (kg) from the literature (Table 4.1). For the extant species, most of the data were obtained from Sillero-Zubiri *et al.* (2004), which provides average body mass for geographically distinct populations of conspecifics, which I averaged to obtain one value per species. For the four extinct species, I used estimates of body mass from Finarelli & Flynn (2006). These estimates come from measurements of the area of the first lower molar (m_1) projected on regression lines calculated from dental area and body mass for extant species. Importantly, these estimates are consistent with other observations for these species, such as estimates of over 60kg for dire wolves based on long bones (Anyonge & Roman, 2006) and the fox-sized skeletal constitution of *H. gregarius* (Wang, 1994). For three of the extant species (indicated in Table 4.1) and all extinct species, body mass data were not separated by sex, and thus I used the combined data for males and females.

Data analysis

Allometric analysis (Huxley, 1924, 1932) assumes that the relationship between trait size (y) and body size (x) varies according to the power law $y = ax^b$, which becomes linear in log scale:

$$\log y = \log a + b \cdot \log x. \tag{4.1}$$

When the allometric slope b is greater than one trait size becomes proportionally larger with increasing body size (positive allometry), while the converse is true when b is lesser than one (negative allometry). The special case of b equal to one is defined as isometry and indicates the maintenance of relative proportions as body size varies. Here, I focus on evolutionary allometry, which compares relative (mean) trait sizes among different species in a group. This is in contrast to static allometry which examines relative trait size among individuals of the same age class within a population, or ontogenetic allometry, which describes the relative growth of a trait during an organism's development (Gould, 1966; Cheverud, 1982; Voje *et al.*, 2014).

To estimate the coefficients of the allometric equation (a and b, equation 1) I used three approaches: *i*) ordinary least squares (OLS) regression on log-log transformed data; *ii*) phylogenetic generalized least squares (PGLS); and, *iii*) ordinary least squares regression on the phylogenetic independent contrasts (PIC) of both variables. The first approach does not correct for phylogenetic non-independence in the data. However, both PGLS and PIC account for phylogenetic relationships to estimate the allometric slope. I used both methods because they provide complementary perspectives on allometry. Specifically, PGLS estimates the intercept (PIC forces the intercept through zero, Garland *et al.*, 1992) but not

Table 4.1: Species included in the study and average measurements. n – number of specimens measured; $\overline{L}(s.d.)$ – Average length of the baculum in millimeters (standard deviation in parentheses); $\overline{\log L}$ – Length measurements were $\log_{10}$ transformed and then averaged; Mass – male body mass in kilograms.

	Species	n	$\overline{L}(s.d.)$	$\overline{\log L}$	Mass
1	*Aelurodon ferox*†	1	118.22 (-)	2.07	35.75 [a]
2	*Aelurodon stirtoni*†	1	117.63 (-)	2.07	26.88 [a]
3	*Aenocyon dirus*†	5	161.11 (23.32)	2.20	63.37 [a]
4	*Atelocynus microtis*	3	60.04 (4.67)	1.78	9.5 [b*]
5	*Canis aureus*	6	57.91 (8.86)	1.76	9.55 [c]
6	*Canis latrans*	10	77.69 (4.45)	1.89	13.94 [e]
7	*Canis lupaster*	4	62.69 (12.08)	1.79	7.0 [d]
8	*Canis lupus*	10	102.55 (9.35)	2.01	45.0 [f]
9	*Canis rufus*	1	112.51 (-)	2.05	28.5 [b]
10	*Cerdocyon thous*	4	53.58 (8.90)	1.72	5.3 [g]
11	*Chrysocyon brachyurus*	2	75.73 (5.91)	1.88	25.0 [b*]
12	*Hesperocyon gregarius*†	1	85.30 (-)	1.93	2.29 [a]
13	*Lupulella adusta*	1	64.53 (-)	1.80	9.4 [b]
14	*Lupulella mesomelas*	3	48.17 (1.17)	1.68	8.1 [b]
15	*Lycalopex culpaeus*	5	63.69 (4.46)	1.80	8.0 [b]
16	*Lycalopex gymnocercus*	3	57.11 (2.99)	1.76	5.25 [b]
17	*Lycalopex sechurae*	4	53.13 (3.68)	1.72	3.6 [b]
18	*Lycaon pictus*	3	105.50 (4.36)	2.02	28 [b]
19	*Nyctereutes procyonoides*	2	52.55 (7.24)	1.72	5.35 [b]
20	*Otocyon megalotis*	4	61.90 (4.96)	1.79	4.0 [b]
21	*Speothos venaticus*	3	68.57 (3.67)	1.84	6.5 [b*]
22	*Urocyon cinereoargenteus*	13	56.91 (4.55)	1.75	4.0 [b]
23	*Urocyon littoralis*	1	50.05 (-)	1.70	2.0 [b]
24	*Vulpes chama*	1	42.90 (-)	1.63	2.8 [b]
25	*Vulpes lagopus*	20	57.55 (5.10)	1.76	3.2 [h]
26	*Vulpes macrotis*	9	43.43 (2.17)	1.64	2.29 [b]
27	*Vulpes rueppellii*	4	37.21 (2.24)	1.57	1.68 [b]
28	*Vulpes velox*	3	40.10 (2.04)	1.60	2.23 [b]
29	*Vulpes vulpes*	7	57.45 (3.53)	1.76	6.3 [b]
30	*Vulpes zerda*	2	30.39 (0.27)	1.48	1.5 [b]

† Extinct species

a - Finarelli & Flynn (2006); b - Sillero-Zubiri *et al.* (2004)
c - Moehlman & Hayssen (2018, Eurasian populations)
d - Moehlman & Hayssen (2018, African populations); e - Bekoff (1977)
f - Macdonald (1984); g - Macdonald & Courtenay (1996)
h - Audet *et al.* (2002); * Combined data for males and females

r^2; in contrast, PIC estimates r^2, but not the intercept. The phylogenies for extant species used here are from Machado (2020), with stem-lineage fossils included following the age and topological uncertainty reported by Slater (2015) and the phylogenetic position of *A. dirus* based on that in Perri *et al.* (2021). Due to uncertainty in phylogenetic relationships among the three subfamilies, as well as uncertainties for node ages for the dire wolf, a total of 18 phylogenies were used (see Chapter 3), although the phylogenetic uncertainty had virtually no impact on the analyses. The analyses were performed in R (R Core Team, 2020, version 4.0.0), using functions from 'ape' (Paradis & Schliep, 2018) and 'nlme' (Pinheiro *et al.*, 2020) for the phylogenetic analyses.

Looking for allometric relationships for measurements with a different number of dimensions changes the value of the slope indicating isometry. Since body mass is volumetric it has three dimensions, while baculum length is unidimensional. To avoid confusion in the interpretation of the allometric slope that may arise from differing numbers of dimensions among variables, I took the cubic root of the body mass before $\log_{10}$ transformation, such that both body mass and baculum length had one dimension in the analysis.

To evaluate the effect of the stem-group fossils on the inferred allometric parameters, I first analyzed just the crown group Caninae (including the dire wolf). Then, I re-analyzed the data but with the addition of the borophagine species and finally, with the further addition of the hesperocyonine species.

4.3 Results

After correction for phylogeny, the allometric slopes for the length of the baculum in the crown group Caninae ranged from 0.91 to 0.92 (for both PGLS and PIC), with r^2 values ranging from 0.73 to 0.74 (for PIC, Table 4.2a). The 95% confidence interval for the allometric slope was 0.69 to 1.16 from PIC estimates and 0.7 to 1.15 from PGLS estimates (Table 4.2a). These values remained largely unchanged after the inclusion of the two species of Borophaginae (Table 4.2b). The addition of the borophagines also had only a minor effect on intercept estimates in the PGLS analyses, changing the intercept from ∼1.53 to 1.57) and slightly widening the confidence interval (Table 4.2a,b).

In contrast, inclusion of *Hesperocyon gregarius* strongly affected intercept estimates, (Figure 4.1a, Table 4.2b,c). The baculum of this extinct species is longer than expected for canids given its body mass and an analysis of the residuals from PGLS models shows that it is the only species that deviates more than two standard deviations from the mean of model residuals. For models without *H. gregarius*, the black-backed jackal (*Lupulella mesomelas*) and the dire wolf (*A. dirus*) deviate the most from the lines of best fit. The black-backed jackal has a smaller baculum relative to body size than other species in the family, and deviates more than two standard deviations from the mean of model residuals (with and without borophagines in the model). In contrast, the dire wolf has a longer baculum for its body size based on the allometric relationship observed for the family. Interestingly, the residuals for the dire wolf baculum are more than two standard deviations from the mean of residuals only

Table 4.2: Parameter estimates from the fitting of the allometric equation (eq. 1) to: (a) the Caninae only (including the extinct dire wolf), (b) the Caninae and two extinct borophagines, (c) the Caninae, borophagines, and hesperocyonine *H. gregarius*. The range of values for parameter estimates for PGLS and PIC derive from the range of possible phylogenies for the taxa, but note the tiny resulting variation (see Figure C.1). C.I. - 95% confidence intervals.

a - Caninae only						
Model	$\log a$	C.I.	b	C.I.	p-val	r^2
OLS	1.507	1.46-1.56	0.993	0.83-1.16	10^{-11}	0.85
PGLS	1.53-1.54	1.44-1.64	0.91-0.92	0.70-1.15	$< 10^{-8}$	-
PICs	-	-	0.91-0.92	0.69-1.16	$< 10^{-8}$	0.73-0.74
b - Caninae and Borophaginae						
Model	$\log a$	C.I.	b	C.I.	p-val	r^2
OLS	1.499	1.45-1.55	1.038	0.88-1.19	10^{-13}	0.87
PGLS	1.57	1.33-1.79	0.91-0.93	0.71-1.14	$< 10^{-8}$	-
PICs	-	-	0.91-0.93	0.70-1.15	$< 10^{-8}$	0.73
c - Caninae, Borophaginae and Hesperocyoninae						
Model	$\log a$	C.I.	b	C.I.	p-val	r^2
OLS	1.532	1.47-1.60	0.961	0.76-1.16	10^{-10}	0.76
PGLS	1.64-1.65	1.44-1.85	0.90-0.91	0.69-1.13	$< 10^{-8}$	-
PICs	-	-	0.87-0.89	0.65-1.12	$< 10^{-8}$	0.70-0.71

when the subfamily Caninae is considered — when borophagines are included, the residuals for the dire wolf are within two standard deviations from the mean of residuals.

For all models, confidence intervals for the estimated allometric slopes included isometry ($b = 1$; Table 4.2). Taking phylogeny into account resulted in a decrease in estimates for the allometric slope and r^2, compared to analyses that did not consider phylogeny. Both phylogenetically informed methods (PGLS and PICs) yielded very similar estimates of allometric slope (Table 4.2).

Parameter estimates were not strongly affected by phylogenetic uncertainty in the relationship among the three canid subfamilies or by the uncertainty in dire wolf divergence time (Figure C.1); accordingly, I arbitrarily chose to present just one regression line in Figure 4.1.

4.4 Discussion

In this chapter, I showed that the length of the baculum of canids displays a steeper slope for evolutionary allometry than has been reported for the order Carnivora as a whole or for mammals in general (Ramm, 2007). The slope for canids is more similar to that for the

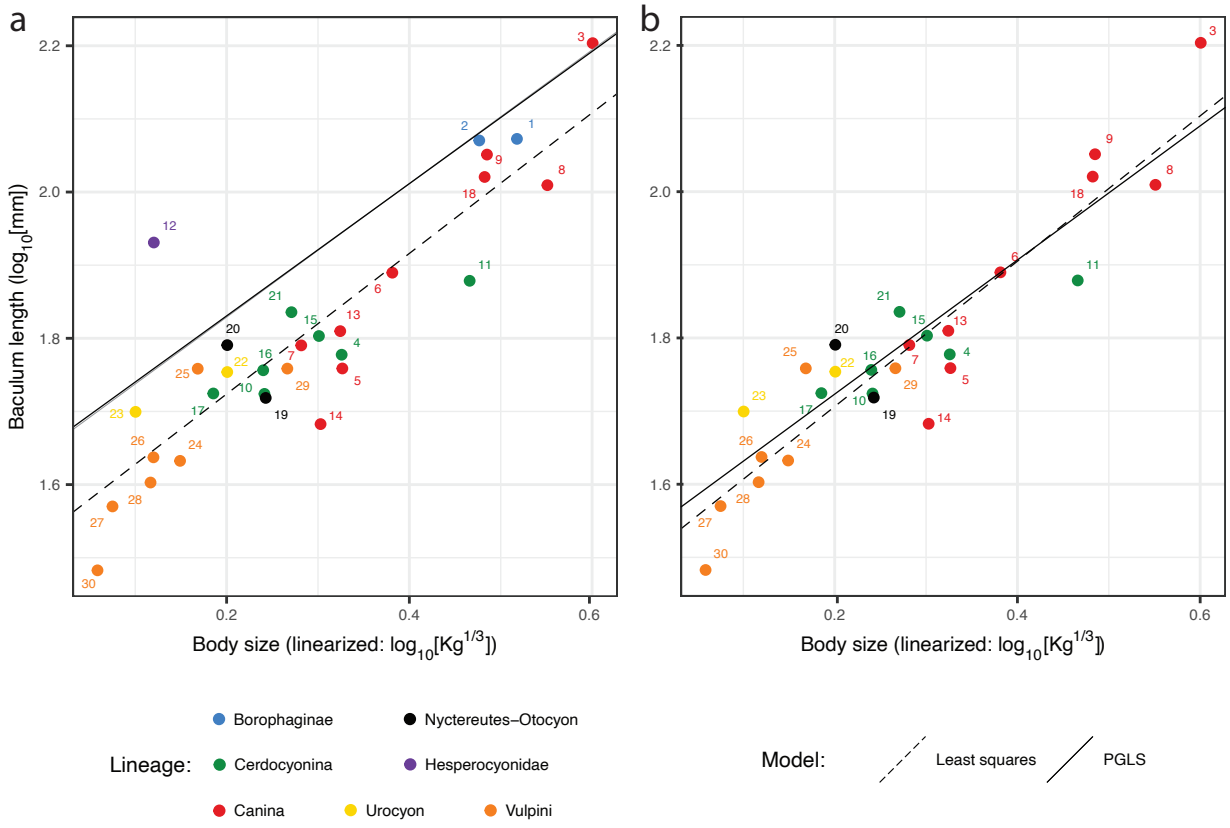

Figure 4.1: Allometric relationships between body size and baculum length. **a:** Lines of best fit for all canids in this study. Note that *Hesperocyon gregarius* (species 12) deviates from all other canids and its inclusion strongly impacts the inferred intercept in the PGLS analysis. **b:** Lines of best fit for crown-group Caninae only, including the extinct dire wolf. Solid lines show PGLS and dashed lines show OLS models. Numbers match species in Table 4.1.

Mustelidae (Baryshnikov *et al.*, 2003). However, the phylogenetically-corrected relationship between body size and baculum length is stronger for canids than for mustelids or any other mammalian lineage, as evidenced by higher values of r^2 (larger than 0.7 in this study, compared with 0.36 for mustelids, although it increases to 0.66 after the exclusion of outliers, Baryshnikov *et al.*, 2003). Thus, body mass is a better predictor of baculum length in canids than in other closely related groups. Contrary to what Ramm (2007) observed for all mammals, these results indicate that the genital size of canids evolves largely isometrically with body mass. In this regard, the baculum of canids diverges from the general pattern described by Eberhard (1985) of male genitalic traits typically evolving more rapidly than other phenotypic traits across multiple animal groups.

It is interesting to note that evolutionary isometry is the predicted outcome if most

species in a group display static isometry (Cheverud, 1982; Voje *et al.*, 2014). The pattern observed here raises the question of whether static isometry could be the rule within multiple species of canines and there is reason to expect static isometry in this group. Kinahan *et al.* (2008) suggested that mating systems are important in determining the nature of the static allometry for mammalian genitalia. More specifically, these authors argue that when mate choice occurs primarily through pre-copulatory strategies, isometry in genital traits is expected, while positive allometry is expected in mammalian species that favor post-copulatory strategies (Kinahan *et al.*, 2008). Given that social monogamy is common in extant canids (Macdonald *et al.*, 2019), it is reasonable to expect that pre-copulatory strategies are prevalent in canids and thus they are likely to display static isometry. Currently, static allometry has been investigated in one species of canid (a population of grey wolves), in which the estimated allometric slope encompasses isometry (the slope $= 1.14 \pm 0.754$, although the uncertainty is large Čanády & Čomor, 2015). Further investigations of static allometry for the length of the baculum of canines could help clarify the relationship between evolutionary and static allometry in this group.

Inferences regarding dire wolves

My analyses demonstrate that the baculum of the dire wolf is proportionally longer than those of extant canids (Figure 4.1b), which confirms and expands previous findings of Hartstone-Rose *et al.* (2015). This difference from the rest of the canine crown group, suggests that this extinct lineage underwent selective pressures for its proportional increase in baculum length. However, it is not known what specific conditions led to the proportional increase in the length of the baculum in dire wolves. Longer bacula have been shown to be correlated with larger testicle mass (Ramm, 2007; Fitzpatrick *et al.*, 2012; Brassey *et al.*, 2020), and thus may be indicative of stronger sperm competition among males (Lüpold *et al.*, 2020). If this functional relationship applies to dire wolves, it suggests that the longer baculum in these animals may be indicative of a non-monogamous mating system in this extinct species.

Previous work on the mating system for the dire wolf has been inconclusive. Van Valkenburgh & Sacco (2002) found that dire wolves may have been slightly more sexually dimorphic than extant canids (based on the coefficient of variation of upper canine teeth). Although this could suggest enhanced competition among males for access to females, Van Valkenburgh & Sacco (2002) did not consider that their evidence was strong enough to conclude a non-monogamous mating system. In contrast, Hartstone-Rose *et al.* (2015) suggested a scenario of strong male-male competition with possible aggression during copulation to explain the larger baculum of dire wolves. Although my results confirm the deviation of the dire wolf baculum from the allometric relationship for other canines, this outcome does not necessarily imply a change in mating system. For example, the black-backed jackal (*L. mesomelas*) has a shorter baculum than expected for its body size, but it is similar to other canines in being socially monogamous (Moehlman, 1983; Walton & Joly, 2003; Macdonald *et al.*, 2019). Thus it is possible that the unusual morphology of the dire wolf baculum may not reflect a change

in mating system.

Inferences for *H. gregarius*

It is striking that *H. gergarius* deviates so much from the allometric curve of other canids. This difference suggests that reproductive strategies for this species may have been different from those of modern canids. In particular, it suggests a scenario of more sperm competition than in living canids, based on relationships between baculum length and testicle mass of modern carnivorans (Ramm, 2007; Fitzpatrick *et al.*, 2012; Brassey *et al.*, 2020). Unfortunately, it is not possible to use this one fossil to make generalizations for the entire subfamily Hesperocyoninae, and more hesperocyonine bacula are needed to understand the allometric curve in this extinct lineage. The description of more hesperocyonine bacula could indicate if there is a different allometric curve for the entire subfamily in comparison to other canids, and whether such difference is due to changes in the allometric slope or allometric intercept.

Evolution of canine bacula

It is generally recognized that the inclusion of fossil data improves ancestral character state reconstruction (Slater *et al.*, 2012). Thus, given the proportion of the bacula of the borophagines, it is tempting to infer that the ancestral trait for the crown group of canines was of a similar proportional size as for the living canids. However, the proportional size of the baculum for total group canids remains unclear because this inference would depend on only two fossil borophagine specimens, long branch lengths between the crown group canids and these fossil taxa (Slater, 2015), and the divergent structure of the hesperocyonine baculum. If the relative baculum size of canines and borophagines is ancestral, it suggests that *H. gregarius* proportionally increased its baculum size. However, given that the phylogenetic position and temporal range of *H. gregarius* are close to the origin of the family (Wang, 1994; Slater, 2015), it is possible that this species had the ancestral condition for the family, in which case the borophagines and canines had a proportional reduction in baculum size. Interestingly, there is a different pattern of evolution between baculum size and baculum shape. The borophagines and *H. gregarius* are more similar in having arched bacula, unlike the essentially straight bacula of crown group canines (Chapter 3). However, the borophagines and canines are more similar to each other than to *Hesperocyon* in terms of relative baculum size. The interplay between shape and relative baculum size in their effect on reproductive strategies remains to be clarified and warrants future research.

Bibliography

Abella, J., A. Valenciano, A. Pérez-Ramos, P. Montoya, & J. Morales, 2013. On the Socio-Sexual Behaviour of the Extinct Ursid Indarctos arctoides: An Approach Based on Its Baculum Size and Morphology. PLoS ONE 8:1–5.

Abramov, A. V., 2000. A taxonomic review of the genus Mustela (Mammalia, Carnivora). Zoosystematica Rossica 8:357–364.

Alcock, J., 1994. Postinsemination associations between males and females in insects: the mate-guarding hypothesis. Annual review of entomology. 39:1–21.

Andersson, K., 2005. Were there pack-hunting canids in the Tertiary, and how can we know? Paleobiology 31:56–72.

André, G. I., R. C. Firman, & L. W. Simmons, 2018. Phenotypic plasticity in genitalia: baculum shape responds to sperm competition risk in house mice. *in* Proceedings of the Royal Society B: Biological Sciences, vol. 285.

———, 2020a. Baculum shape and paternity success in house mice: evidence for genital coevolution. Philosophical Transactions of the Royal Society B: Biological Sciences 375:20200150.

———, 2020b. The coevolution of male and female genitalia in a mammal: A quantitative genetic insight. Evolution 74:1558–1567.

———, 2021. The effect of baculum shape and mating behavior on mating-induced prolactin release in female house mice. Behavioral Ecology 32:1192–1201.

Anyonge, W. & C. Roman, 2006. New body mass estimates for Canis dirus, the extinct Pleistocene dire wolf. Journal of Vertebrate Paleontology 26:209–212.

Arnqvist, G. & L. Rowe, 2005. Sexual Conflict. Princeton University Press, Princeton, New Jersey.

Asa, C. S. & C. Valdespino, 1998. Canid reproductive biology: An integration of proximate mechanisms and ultimate causes. American Zoologist 38:251–259.

Audet, A. M., C. B. Robbins, & S. Larivière, 2002. Alopex lagopus. Mammalian Species 713:1–10.

Bapst, D. W., 2014. Assessing the effect of time-scaling methods on phylogeny-based analyses in the fossil record. Paleobiology 40:331–351.

Baryshnikov, G. F., O. R. P. Bininda-Emonds, & A. V. Abramov, 2003. Morphological variability and evolution of the baculum (os penis) in Mustelidae (Carnivora). Journal of Mammalogy 84:673–690.

Bekoff, M., 1977. Canis latrans. Mammalian Species P. 1.

Best, T. L. & G. D. Schnell, 1974. Bacular Variation in Kangaroo Rats (Genus Dipodomys). American Midland Naturalist 91:257.

Bonhomme, V., S. Picq, C. Gaucherel, & J. Claude, 2014. Momocs: Outline analysis using R. Journal of Statistical Software 56:1–24.

Bookstein, F. L., 1992. Morphometric Tools for Landmark Data: Geometry and Biology. Cambridge University Press.

Boucot, A. J. & G. O. Poinar Jr., 2010. Fossil Behavior Compendium. First edit ed. CRC Press.

Brassey, C. A., J. Behnsen, & J. D. Gardiner, 2020. Postcopulatory sexual selection and the evolution of shape complexity in the carnivoran baculum. Proceedings of the Royal Society B: Biological Sciences 287:20201883.

Brassey, C. A., J. D. Gardiner, & A. C. Kitchener, 2018. Testing hypotheses for the function of the carnivoran baculum using finite-element analysis. Proceedings of the Royal Society B: Biological Sciences 285.

Brennan, P. L., C. J. Clark, & R. O. Prum, 2010. Explosive eversion and functional morphology of the duck penis supports sexual conflict in waterfowl genitalia. Proceedings of the Royal Society B: Biological Sciences 277:1309–1314.

Brennan, P. L. & R. O. Prum, 2015. Mechanisms and evidence of genital coevolution: The roles of natural selection, mate choice, and sexual conflict. Cold Spring Harbor Perspectives in Biology 7:1–21.

Brennan, P. L., R. O. Prum, K. G. McCracken, M. D. Sorenson, R. E. Wilson, & T. R. Birkhead, 2007. Coevolution of male and female genital morphology in waterfowl. PLoS ONE 2.

Brindle, M. & C. Opie, 2016. Postcopulatory sexual selection influences baculum evolution in primates and carnivores. Proceedings of the Royal Society of London B: Biological Sciences 283.

Burt, W., 1960. Bacula of North American Mammals. Miscellaneous Publications Museum of Zoology, University of Michigan .

Burt, W. H., 1936. A Study of the Baculum in the Genera Perognathus and Dipodomys. Journal of Mammalogy 17:145.

Bush, A. M., G. Hunt, & R. K. Bambach, 2016. Sex and the shifting biodiversity dynamics of marine animals in deep time. Proceedings of the National Academy of Sciences of the United States of America 113:14073–14078.

Čanády, A., 2013. Variability of the baculum in the red fox (Vulpes vulpes) from Slovakia. Zoology and Ecology 23:165–170.

Čanády, A. & L. Čomor, 2015. Allometry of the baculum in the Wolf (Canis lupus, Canidae) as an indicator of viability and quality in males. Zoology and Ecology 25:192–198.

Chaine, J., 1926. L'os pénien étude descriptive et comparative. Actes de la Société linnéenne de Bordeaux 78:5–195.

Cheverud, J. M., 1982. Relationships among ontogenetic, static, and evolutionary allometry. American Journal of Physical Anthropology 59:139–149.

Crampton, J. S., 1995. Elliptic Fourier shape analysis of fossil bivalves: some practical considerations. Lethaia 28:179–186.

Csanády, A., S. Duranková, & E. Labancová, 2019. Are baculum size and allometry a response to post-copulatory sexual selection in promiscuous males of the house mouse? Zoomorphology 138:287–296.

Didier, R., 1946. Etude Systematique de l'os penien des Mammiferes. Ordre des Carnivores 1. Famille des canidés. Mammalia 10:80–91.

———, 1948. Etude systématique de l'os penien des mammifères. Mammalia 12:67–93.

———, 1949. Etude systematique de l'os penien des Mammiferes: Famille des félidés. Mammalia 13:17–37.

Dixson, A., J. Nyholt, & M. Anderson, 2004. A positive relationship between baculum length and prolonged intromission patterns in mammals. Acta Zoologica Sinica 50:490–503.

Dixson, A. F., 1987a. Baculum length and copulatory behavior in primates. American Journal of Primatology 13:51–60.

———, 1987b. Observations on the evolution of the genitalia and copulatory behaviour in male primates. Journal of Zoology 213:423–443.

———, 1995. Baculum length and copulatory behaviour in carnivores and pinnipeds (Grand Order Ferae). Journal of Zoology 235:67–76.

Dundas, R. G., 1999. Quaternary records of the dire wolf, Canis dirus, in North and South America. Boreas 28:375–385.

Eberhard, W., 1996. Female control: sexual selection by cryptic female choice. Princeton University Press, Princeton, New Jersey.

Eberhard, W. G., 1985. Sexual Selection and Animal Genitalia. Harvard University Press, Cambridge, MA (U.S.A.) and London, England.

Elder, W. H., 1951. The Baculum as an Age Criterion in Mink. Journal of Mammalogy 32:43.

Enders, R. K., 1952. Reproduction in the mink (\textit{Mustela vison}). Proceedings of the American Philosophical Society 96:691–755.

Fay, F. H., 1982. Ecology and Biology of the Pacific Walrus, Odobenus rosmarus divergens Illiger. North American Fauna 74:1–279.

Ferguson, S. H. & S. Larivière, 2004. Are long penis bones an adaption to high latitude snowy environments? Oikos 105:255–267.

Finarelli, J. A. & J. J. Flynn, 2006. Ancestral state reconstruction of body size in the Caniformia (Carnivora, mammalia): The effects of incorporating data from the fossil record. Systematic Biology 55:301–313.

Fischer, T. C. & M. K. Hörnig, 2019. Mating moths (Tineidae, ditrysia, lepidoptera) preserved as frozen behavior inclusion in baltic amber (eocene). Palaeontologia Electronica 22:1–10.

Fitzpatrick, J. L., M. Almbro, A. Gonzalez-Voyer, N. Kolm, & L. W. Simmons, 2012. Male Contest Competition And The Coevolution Of Weaponry And Testes In Pinnipeds. Evolution 66:3595–3604.

Friley, C. E., 1949. Age Determination, by Use of the Baculum, in the River Otter, Lutra c. canadensis Schreber. Journal of Mammalogy 30:102.

Gardiner, J. D., J. Behnsen, & C. A. Brassey, 2018. Alpha shapes: Determining 3D shape complexity across morphologically diverse structures. BMC Evolutionary Biology 18:1–16.

Garland, T., P. H. Harvey, & A. R. Ives, 1992. Procedures for the Analysis of Comparative Data Using Phylogenetically Independent Contrasts. Systematic Biology 41:18.

Gonçalves, T. C., D. F. de Sousa, M. P. E. Pinto, R. A. R. Rodrigues, E. G. Giese, É. Branco, & A. R. de Lima, 2022. Morphology of the male reproductive tract of Eira barbara. Journal of Veterinary Medicine Series C: Anatomia Histologia Embryologia Pp. 1–10.

Good, J. M., J. R. Demboski, D. W. Nagorsen, & J. Sullivan, 2003. Phylogeography and introgressive hybridization: Chipmunks (genus Tamias) in the northern Rocky Mountains. Evolution 57:1900–1916.

Gopalakrishnan, S., M. H. S. Sinding, J. Ramos-Madrigal, J. Niemann, J. A. Samaniego Castruita, F. G. Vieira, C. Carøe, M. d. M. Montero, L. Kuderna, A. Serres, V. M. González-Basallote, Y. H. Liu, G. D. Wang, T. Marques-Bonet, S. Mirarab, C. Fernandes, P. Gaubert, K. P. Koepfli, J. Budd, E. K. Rueness, M. P. Heide-Jørgensen, B. Petersen, T. Sicheritz-Ponten, L. Bachmann, Ø. Wiig, A. J. Hansen, & M. T. P. Gilbert, 2018. Interspecific Gene Flow Shaped the Evolution of the Genus Canis. Current Biology 28:3441–3449.e5.

Gould, S. J., 1966. Allometry and size in ontogeny and phylogeny. Biological reviews of the Cambridge Philosophical Society 41:587–640.

Harrison, J. A., 1982. The Baculum of Plesiogulo (Carnivora: Mustelidae). Journal of Paleontology 56:1266–1273.

Hartstone-Rose, A., R. G. Dundas, B. Boyde, R. C. Long, A. B. Farrell, & C. A. Shaw, 2015. The Bacula of Rancho La Brea. Natural History Museum of Los Angeles County Science Series 42:53–63.

Hatcher, J. B., 1902. Oligocene Canidae. Memoirs of the Carnegie Museum 1:65–108.

Heldstab, S. A., D. W. Müller, S. M. Graber, L. Bingaman Lackey, E. Rensch, J. M. Hatt, P. Zerbe, & M. Clauss, 2018. Geographical Origin, Delayed Implantation, and Induced Ovulation Explain Reproductive Seasonality in the Carnivora. Journal of Biological Rhythms 33:402–419.

Herdina, A. N., B. Herzig-Straschil, H. Hilgers, B. D. Metscher, & H. Plenk, 2010. Histomorphology of the penis bone (baculum) in the gray long-eared bat Plecotus austriacus (Chiroptera, Vespertilionidae). Anatomical Record 293:1248–1258.

Herdina, A. N., D. A. Kelly, H. Jahelková, P. H. Lina, I. Horáček, & B. D. Metscher, 2015. Testing hypotheses of bat baculum function with 3D models derived from microCT. Journal of Anatomy 226:229–235.

Hildebrand, M., 1951. Morphology of the skeleton and integument in recent canidae. Ph.D. thesis, Univ. of California, Berkeley.

Hosken, D. J., K. E. Jones, K. Chipperfield, & A. Dixson, 2001. Is the bat os penis sexually selected? Behavioral Ecology and Sociobiology 50:450–460.

Hosken, D. J. & P. Stockley, 2004. Sexual selection and genital evolution. Trends in Ecology and Evolution 19:87–93.

Hsieh, S. & R. E. Plotnick, 2020. The representation of animal behaviour in the fossil record. Animal Behaviour 169:65–80.

Huxley, J. S., 1924. Constant Differential Growth-Ratios and their Significance. Nature 114:895–896.

———, 1932. Problems of Relative Growth. L. MacVeagh, The Dial Press, New York.

Kelly, D. A., 2000. Anatomy of the baculum-corpus cavernosum interface in the norway rat (Rattus norvegicus), and implications for force transfer during copulation. Journal of morphology 244:69–77.

Kinahan, A. A., N. C. Bennett, L. E. Belton, & P. W. Bateman, 2008. Do mating strategies determine genital allometry in African mole rats (Bathyergidae)? Journal of Zoology 274:312–317.

Kinahan, A. A., N. C. Bennett, M. J. O'Riain, L. Hart, & P. W. Bateman, 2007. Size matters: Genital allometry in an African mole-rat (Family: Bathyergidae). Evolutionary Ecology 21:201–213.

Kleiman, D. G., 1968. reproduction in the Canidae. International Zoo Yearbook 8:3–8.

Koepfli, K. P., J. Pollinger, R. Godinho, J. Robinson, A. Lea, S. Hendricks, R. M. Schweizer, O. Thalmann, P. Silva, Z. Fan, A. A. Yurchenko, P. Dobrynin, A. Makunin, J. A. Cahill, B. Shapiro, F. Álvares, J. C. Brito, E. Geffen, J. A. Leonard, K. M. Helgen, W. E. Johnson, S. J. O'Brien, B. Van Valkenburgh, & R. K. Wayne, 2015. Genome-wide evidence reveals that African and Eurasian golden jackals are distinct species. Current Biology 25:2158–2165.

Lamarca, A. P. & C. G. Schrago, 2020. Fast speciations and slow genes: Uncovering the root of living canids. Biological Journal of the Linnean Society 129:492–504.

Larivière, S. & S. H. Ferguson, 2002. On the evolution of the mammalian baculum: Vaginal friction, prolonged intromission or induced ovulation? Mammal Review 32:283–294.

———, 2003. Evolution of induced ovulation in North American carnivores. Journal of Mammalogy 84:937–947.

Long, C. & T. Frank, 1968. Morphometric Variation and Function in the Baculum, with Comments on Correlation of Parts. Journal of Mammalogy 49:32–43.

Long, C. A., 1969. Gross morphology of the penis in seven species of the mustelidae. Mammalia 33:145–160.

Lüpold, S., R. A. De Boer, J. P. Evans, J. L. Tomkins, & J. L. Fitzpatrick, 2020. How sperm competition shapes the evolution of testes and sperm: A meta-analysis: Sperm competition meta-analysis. Philosophical Transactions of the Royal Society B: Biological Sciences 375.

Macdonald, D., 1984. The Encyclopedia of Mammals. Facts on File, New York, NY.

Macdonald, D. W., L. A. Campbell, J. F. Kamler, J. Marino, G. Werhahn, & C. Sillero-Zubiri, 2019. Monogamy: Cause, Consequence, or Corollary of Success in Wild Canids?

Macdonald, D. W. & O. Courtenay, 1996. Enduring social relationships in a population of crab-eating zorros, Cerdocyon thous, in Amazonian Brazil (Carnivora, Canidae). Journal of Zoology 239:329–355.

Machado, F. A., 2020. Selection and constraints in the ecomorphological adaptive evolution of the skull of living canidae (Carnivora, mammalia). American Naturalist 196:197–215.

Mayr, E., 1963. Animal Species and Evolution. Harvard University Press, Cambridge, MA (U.S.A.).

Moehlman, P. D., 1983. Socioecology of silverbacked and golden jackals (Canis mesomelas and Canis aureus). Advances in the study of mammalian behavior 7:423–453.

Moehlman, P. D. & V. Hayssen, 2018. Canis aureus (Carnivore: Canidae). Mammalian Species 50:14–25.

Morejohn, G. V., 1975. A phylogeny of otariid seals based on morphology of the baculum. Rapports et Proces-Verbaux des Reunions (Denmark) .

Munthe, K., 1989. The skeleton of the Borophaginae (Carnivora, Canidae): morphology and function, vol. 133. Univ of California Press.

Olsen, S. J., 1959. The baculum of the Miocene carnivore Amphicyon. Journal of Paleontology 33:449–450.

Orr, T. J. & P. L. R. Brennan, 2016. All Features Great and Small—the Potential Roles of the Baculum and Penile Spines in Mammals. Integrative and Comparative Biology 56:635–643.

Packard, R., 1960. Speciation and Evolution of the Pygmy Mice, Genus Baiomys. University of Kansas Publications Museum of Natural History 9:579–670.

Paradis, E. & K. Schliep, 2018. ape 5.0: an environment for modern phylogenetics and evolutionary analyses in R. Bioinformatics 35:526–528.

Parker, G. A., 1970. Sperm competition and its evolutionary consequences in the insects. Biological Reviews 45:525–567.

———, 1979. Sexual selection and sexual conflict. Sexual selection and reproductive competition in insects P. 123:166.

Parker, G. A. & T. Pizzari, 2010. Sperm competition and ejaculate economics. Biological Reviews 85:897–934.

Paterson, R. S., N. Rybczynski, N. Kohno, & H. C. Maddin, 2020. A Total Evidence Phylogenetic Analysis of Pinniped Phylogeny and the Possibility of Parallel Evolution Within a Monophyletic Framework. Frontiers in Ecology and Evolution 7.

Patterson, B. D., 1983. Baculum-Body Size Relationships as Evidence for a Selective Continuum on Bacular Morphology. Journal of Mammalogy 64:496–499.

Patterson, B. D. & C. S. Thaeler, 1982. The Mammalian Baculum: Hypotheses on the Nature of Bacular Variability. Journal of Mammalogy 63:1–15.

Pennell, M. W., J. M. Eastman, G. J. Slater, J. W. Brown, J. C. Uyeda, R. G. Fitzjohn, M. E. Alfaro, & L. J. Harmon, 2014. Geiger v2.0: An expanded suite of methods for fitting macroevolutionary models to phylogenetic trees. Bioinformatics 30:2216–2218.

Perini, F. A., C. A. M. Russo, & C. G. Schrago, 2010. The evolution of South American endemic canids: A history of rapid diversification and morphological parallelism. Journal of Evolutionary Biology 23:311–322.

Perri, A. R., K. J. Mitchell, A. Mouton, S. Álvarez-Carretero, A. Hulme-Beaman, J. Haile, A. Jamieson, J. Meachen, A. T. Lin, B. W. Schubert, C. Ameen, E. E. Antipina, P. Bover, S. Brace, A. Carmagnini, C. Carøe, J. A. Samaniego Castruita, J. C. Chatters, K. Dobney, M. dos Reis, A. Evin, P. Gaubert, S. Gopalakrishnan, G. Gower, H. Heiniger, K. M. Helgen, J. Kapp, P. A. Kosintsev, A. Linderholm, A. T. Ozga, S. Presslee, A. T. Salis, N. F. Saremi, C. Shew, K. Skerry, D. E. Taranenko, M. Thompson, M. V. Sablin, Y. V. Kuzmin, M. J. Collins, M. H. S. Sinding, M. T. P. Gilbert, A. C. Stone, B. Shapiro, B. Van Valkenburgh, R. K. Wayne, G. Larson, A. Cooper, & L. A. Frantz, 2021. Dire wolves were the last of an ancient New World canid lineage. Nature 591:87–91.

Peterson, O. A., 1910. Description of new carnivores from the Miocene of western Nebraska. Mem. of the Carnegie Museum 4:205–278.

Pinheiro, J., D. Bates, S. DebRoy, D. Sarkar, & R Core Team, 2020. {nlme}: Linear and Nonlinear Mixed Effects Models.

Pocock, R., 1918. The baculum or os penis of some genera of Mustelidæ. Annals and Magazine of Natural History 1:307–312.

Pocock, R. I., 1923. The Classification of the Sciuridae. Proceedings of the Zoological Society of London 93:209–246.

Pohl, L., 1911. Das Os Penis der Carnivoren einschliesslich der Pinnipedier. Jenaische Zeitschrift fuer Naturwissenschaft 47:115–160.

Porto, L. M. V., R. Maestri, & L. Da Silva Duarte, 2019. Evolutionary relationships among life-history traits in Caninae (Mammalia: Carnivora). Biological Journal of the Linnean Society 128:311–322.

R Core Team, 2020. R: A Language and Environment for Statistical Computing. R Foundation for Statistical Computing, Vienna, Austria.

Ramm, S. A., 2007. Sexual selection and genital evolution in mammals: A phylogenetic analysis of baculum length. American Naturalist 169:360–369.

Revell, L. J., 2012. phytools: An R package for phylogenetic comparative biology (and other things). Methods in Ecology and Evolution 3:217–223.

Schultz, N. G., J. Ingels, A. Hillhouse, K. Wardwell, P. L. Chang, J. M. Cheverud, C. Lutz, L. Lu, R. W. Williams, & M. D. Dean, 2016a. The genetic basis of baculum size and shape variation in mice. G3: Genes, Genomes, Genetics 6:1141–1151.

Schultz, N. G., M. Lough-Stevens, E. Abreu, T. Orr, & M. D. Dean, 2016b. The Baculum was Gained and Lost Multiple Times during Mammalian Evolution. Integrative and Comparative Biology 56:644–656.

Scott, W. B. & G. L. Jepsen, 1936. The Mammalian Fauna of the White River Oligocene: Part I. Insectivora and Carnivora. Transactions of the American Philosophical Society 28:1.

Sharir, A., D. Israeli, J. Milgram, J. D. Currey, E. Monsonego-Ornan, & R. Shahar, 2011. The canine baculum: The structure and mechanical properties of an unusual bone. Journal of Structural Biology 175:451–456.

Sillero-Zubiri, C., M. Hoffmann, & D. W. MacDonald, 2004. Canids : foxes, wolves, jackals and dogs. Status survey and conservation action plan. Gland, Switzerland and Cambridge, UK.

Silvestro, D., A. Antonelli, N. Salamin, & T. B. Quental, 2015. The role of clade competition in the diversification of North American canids. Proceedings of the National Academy of Sciences 112:8684–8689.

Simmons, L. W., 2014. Sexual selection and genital evolution. Austral Entomology 53:1–17.

Simmons, L. W. & R. C. Firman, 2014. Experimental evidence for the evolution of the mammalian baculum by sexual selection. Evolution 68:276–283.

Slater, G. J., 2015. Iterative adaptive radiations of fossil canids show no evidence for diversity-dependent trait evolution. Proceedings of the National Academy of Sciences 112:4897–4902.

Slater, G. J. & A. R. Friscia, 2019. Hierarchy in adaptive radiation: A case study using the Carnivora (Mammalia). Evolution 73:524–539.

Slater, G. J., L. J. Harmon, & M. E. Alfaro, 2012. INTEGRATING FOSSILS WITH MOLECULAR PHYLOGENIES IMPROVES INFERENCE OF TRAIT EVOLUTION. Evolution 66:3931–3944.

Spani, F., M. P. Morigi, M. Bettuzzi, M. Scalici, G. Gentile, & M. Carosi, 2021. The ultimate database to (re)set the evolutionary history of primate genital bones. Scientific Reports 11:1–15.

Stockley, P., 2012. The baculum. Current Biology 22:1032–1033.

Stockley, P., S. A. Ramm, A. L. Sherborne, M. D. F. Thom, S. Paterson, & J. L. Hurst, 2013. Baculum morphology predicts reproductive success of male house mice under sexual selection. BMC Biology 11:1–6.

Tedford, R. H., W. Xiaoming, & B. E. Taylor, 2009. Phylogenetic systematics of the North American fossil caninae (Carnivora: Canidae). Bulletin of the American Museum of Natural History Pp. 1–218.

Thornhill, R., 1983. Cryptic female choice and its implications in the scorpionfly Harpobittacus nigriceps. American Naturalist 122:765–788.

Tomiya, S. & Z. J. Tseng, 2016. Whence the beardogs? Reappraisal of the middle to late eocene 'miacis' from Texas, USA, and the origin of amphicyonidae (mammalia, carnivora). Royal Society Open Science 3.

Van Valkenburgh, B. & T. Sacco, 2002. Sexual dimorphism, social behavior, and intrasexual competition in large pleistocene carnivorans. Journal of Vertebrate Paleontology 22:164–169.

Van Valkenburgh, B., T. Sacco, & X. Wang, 2003. Pack hunting in Miocene borophagine dogs: Evidence from craniodental morphology and body size. Bulletin of the American Museum of Natural History 2003:147–162.

Verrell, P. A., 1992. Primate Penile Morphologies and Social Systems: Further Evidence for an Association. Folia Primatologica 59:114–120.

Voje, K. L., T. F. Hansen, C. K. Egset, G. H. Bolstad, & C. Pélabon, 2014. Allometric constraints and the evolution of allometry. Evolution 68:866–885.

VonHoldt, B. M., J. A. Cahill, Z. Fan, I. Gronau, J. Robinson, J. P. Pollinger, B. Shapiro, J. Wall, & R. K. Wayne, 2016. Whole-genome sequence analysis shows that two endemic species of North American Wolf are admixtures of the coyote and gray Wolf. Science Advances 2:1–14.

Waage, J. K., 1979. Dual function of the damselfly penis: Sperm removal and transfer. Science 203:916–918.

Walton, L. R. & D. O. Joly, 2003. Canis mesomelas. Mammalian Species 715:1–9.

Wang, X., 1994. Phylogenetic Systematics of the Hesperocyoninae (Carnivora:Canidae). Bulletin of the American Museum of Natural HIstory .

Wang, X., M. F. Teaford, & B. E. Taylor, 1999. Systematics of Borophaginae. Bulletin of the American Museum of Natural History 243:1–391.

Wayne, R. K., E. Geffen, D. J. Girman, K. P. Koepfli, L. M. Lau, & C. R. Marshall, 1997. Molecular systematics of the Canidae. Systematic Biology 46:622–646.

Weimann, B., M. A. Edwards, & C. N. Jass, 2014. Identification of the baculum in American pika (Ochotona princeps: Lagomorpha) from southwestern Alberta, Canada. Journal of Mammalogy 95:284–289.

White, J., 1953. The Baculum in the Chipmunks of Western North America. University of Kansas Publications, Museum of Natural History 5:611–631.

Wright, P. L., 1947. The Sexual Cycle of the Male Long-Tailed Weasel (Mustela frenata). Journal of Mammalogy 28:343.

Wyss, A. R. & J. J. Flynn, 1993. A phylogenetic analysis and definition of the Carnivora. chap. Chapter 4, Pp. 32–52, *in* F. Szalay, M. Novacek, & M. McKenna, eds. Mammal Phylogeny: Placentals. Springer Verlag, New York, New York.

Zrzavý, J., P. Duda, J. Robovský, I. Okřinová, & V. Pavelková Řičánková, 2018. Phylogeny of the Caninae (Carnivora): Combining morphology, behaviour, genes and fossils. Zoologica Scripta 47:373–389.

Appendix A

Specimens observed

Museum	SpecNum	Lineage	Genus	Species	OBS
AMNHFAM	61723	Borophaginae	Aelurodon	ferox	[1]
USNMVP	215320	Borophaginae	Aelurodon	stirtoni	[2]
LACMHCPP	8638	Canina	Aenocyon	dirus	[3]
LACMHCPP	8650	Canina	Aenocyon	dirus	[3]
LACMHCPP	8854	Canina	Aenocyon	dirus	[3]
LACMHCPP	9009	Canina	Aenocyon	dirus	[3]
UCMP	999999	Canina	Aenocyon	dirus	XXX[4]
AMNHM	100095	Cerdocyonina	Atelocynus	microtis	[5]
FMNH	93955	Cerdocyonina	Atelocynus	microtis	[5]
FMNH	121286	Cerdocyonina	Atelocynus	microtis	[5]
FMNH	57264	Canina	Canis	aureus	
FMNH	112364	Canina	Canis	aureus	
FMNH	112366	Canina	Canis	aureus	
FMNH	112367	Canina	Canis	aureus	[6]
FMNH	112369	Canina	Canis	aureus	[6]
FMNH	112371	Canina	Canis	aureus	
MVZ	19035	Canina	Canis	latrans	
MVZ	19132	Canina	Canis	latrans	
MVZ	25553	Canina	Canis	latrans	
MVZ	35447	Canina	Canis	latrans	
MVZ	74824	Canina	Canis	latrans	
MVZ	78410	Canina	Canis	latrans	
MVZ	80757	Canina	Canis	latrans	
MVZ	83446	Canina	Canis	latrans	
MVZ	83447	Canina	Canis	latrans	
MVZ	230266	Canina	Canis	latrans	
AMNHM	27741	Canina	Canis	lupaster	
FMNH	79804	Canina	Canis	lupaster	
FMNH	105807	Canina	Canis	lupaster	

FMNH	106722	Canina	Canis	lupaster	
FMNH	51772	Canina	Canis	lupus	
FMNH	54203	Canina	Canis	lupus	[5]
FMNH	119851	Canina	Canis	lupus	
MVZ	74828	Canina	Canis	lupus	
MVZ	119675	Canina	Canis	lupus	
MVZ	119677	Canina	Canis	lupus	
MVZ	119811	Canina	Canis	lupus	
MVZ	129254	Canina	Canis	lupus	
USNM	349918	Canina	Canis	lupus	
USNM	529683	Canina	Canis	lupus	
MVZ	120931	Canina	Canis	rufus	[5]
FMNH	68891	Cerdocyonina	Cerdocyon	thous	
FMNH	68893	Cerdocyonina	Cerdocyon	thous	
MVZ	145330	Cerdocyonina	Cerdocyon	thous	
MVZ	145332	Cerdocyonina	Cerdocyon	thous	
AMNHM	133941	Cerdocyonina	Chrysocyon	brachyurus	
MVZ	119566	Cerdocyonina	Chrysocyon	brachyurus	[5]
MCZ	3667	Hesperocyoninae	Hesperocyon	gregarius	[7]
AMNHM	33322	Canina	Lupulella	adusta	
FMNH	66873	Canina	Lupulella	mesomelas	
FMNH	73038	Canina	Lupulella	mesomelas	
USNM	296091	Canina	Lupulella	mesomelas	
FMNH	52499	Cerdocyonina	Lycalopex	culpaeus	
FMNH	52500	Cerdocyonina	Lycalopex	culpaeus	
FMNH	78660	Cerdocyonina	Lycalopex	culpaeus	
FMNH	78663	Cerdocyonina	Lycalopex	culpaeus	
MVZ	116204	Cerdocyonina	Lycalopex	culpaeus	
AMNHM	205754	Cerdocyonina	Lycalopex	gymnocercus	
AMNHM	205761	Cerdocyonina	Lycalopex	gymnocercus	
AMNHM	205763	Cerdocyonina	Lycalopex	gymnocercus	
FMNH	80958	Cerdocyonina	Lycalopex	sechurae	
FMNH	80965	Cerdocyonina	Lycalopex	sechurae	
FMNH	80967	Cerdocyonina	Lycalopex	sechurae	
FMNH	80969	Cerdocyonina	Lycalopex	sechurae	
AMNHM	70443	Canina	Lycaon	pictus	
FMNH	153720	Canina	Lycaon	pictus	[5]
USNM	296104	Canina	Lycaon	pictus	
AMNHM	57113	Nyctereutes-Otocyon	Nyctereutes	procyonoides	
MVZ	119062	Nyctereutes-Otocyon	Nyctereutes	procyonoides	
AMNHM	63993	Nyctereutes-Otocyon	Otocyon	megalotis	
FMNH	73040	Nyctereutes-Otocyon	Otocyon	megalotis	
FMNH	73041	Nyctereutes-Otocyon	Otocyon	megalotis	
FMNH	123656	Nyctereutes-Otocyon	Otocyon	megalotis	[5]

AMNHM	167846	Cerdocyonina	Speothos	venaticus
MVZ	126276	Cerdocyonina	Speothos	venaticus
MVZ	184054	Cerdocyonina	Speothos	venaticus
MVZ	2328	Urocyon	Urocyon	cinereoargenteus
MVZ	31994	Urocyon	Urocyon	cinereoargenteus
MVZ	32441	Urocyon	Urocyon	cinereoargenteus
MVZ	35441	Urocyon	Urocyon	cinereoargenteus
MVZ	81325	Urocyon	Urocyon	cinereoargenteus
MVZ	82160	Urocyon	Urocyon	cinereoargenteus
MVZ	82161	Urocyon	Urocyon	cinereoargenteus
MVZ	98300	Urocyon	Urocyon	cinereoargenteus
MVZ	122806	Urocyon	Urocyon	cinereoargenteus
MVZ	132050	Urocyon	Urocyon	cinereoargenteus
MVZ	149768	Urocyon	Urocyon	cinereoargenteus
MVZ	184057	Urocyon	Urocyon	cinereoargenteus
MVZ	230248	Urocyon	Urocyon	cinereoargenteus
MVZ	38929	Urocyon	Urocyon	littoralis
USNM	296103	Vulpini	Vulpes	chama
MVZ	46713	Vulpini	Vulpes	lagopus
MVZ	123987	Vulpini	Vulpes	lagopus
MVZ	125609	Vulpini	Vulpes	lagopus
MVZ	184038	Vulpini	Vulpes	lagopus
MVZ	206554	Vulpini	Vulpes	lagopus
MVZ	206555	Vulpini	Vulpes	lagopus
MVZ	206566	Vulpini	Vulpes	lagopus
MVZ	206602	Vulpini	Vulpes	lagopus
MVZ	206644	Vulpini	Vulpes	lagopus
MVZ	206661	Vulpini	Vulpes	lagopus
MVZ	206686	Vulpini	Vulpes	lagopus
MVZ	206687	Vulpini	Vulpes	lagopus
MVZ	206688	Vulpini	Vulpes	lagopus
MVZ	206690	Vulpini	Vulpes	lagopus
MVZ	206691	Vulpini	Vulpes	lagopus
MVZ	206694	Vulpini	Vulpes	lagopus
MVZ	206697	Vulpini	Vulpes	lagopus
MVZ	206699	Vulpini	Vulpes	lagopus
MVZ	206702	Vulpini	Vulpes	lagopus
MVZ	234370	Vulpini	Vulpes	lagopus
MVZ	10583	Vulpini	Vulpes	macrotis
MVZ	195365	Vulpini	Vulpes	macrotis
MVZ	195372	Vulpini	Vulpes	macrotis
MVZ	195373	Vulpini	Vulpes	macrotis
MVZ	206994	Vulpini	Vulpes	macrotis
MVZ	207003	Vulpini	Vulpes	macrotis

MVZ	207004	Vulpini	Vulpes	macrotis
MVZ	207014	Vulpini	Vulpes	macrotis
MVZ	224402	Vulpini	Vulpes	macrotis
FMNH	106388	Vulpini	Vulpes	rueppellii
FMNH	106401	Vulpini	Vulpes	rueppellii
FMNH	140152	Vulpini	Vulpes	rueppellii
USNM	601446	Vulpini	Vulpes	rueppellii
AMNHM	100125	Vulpini	Vulpes	velox
FMNH	137317	Vulpini	Vulpes	velox
FMNH	137318	Vulpini	Vulpes	velox
MVZ	46781	Vulpini	Vulpes	vulpes
MVZ	123988	Vulpini	Vulpes	vulpes
MVZ	222279	Vulpini	Vulpes	vulpes
MVZ	222308	Vulpini	Vulpes	vulpes
MVZ	222313	Vulpini	Vulpes	vulpes
MVZ	222323	Vulpini	Vulpes	vulpes
MVZ	222343	Vulpini	Vulpes	vulpes
FMNH	140196	Vulpini	Vulpes	zerda
FMNH	140201	Vulpini	Vulpes	zerda

[1]Portions that are broken and missing left incomplete
[2]Skeleton mount edited out in photoshop for outline
[3]From Hartstone-rose et al 2015
[4]Needs new specimen number
[5]Zoo specimen
[6]Specimens FMNH 112369 and 112367 are stored together
[7]Using outline published in Wang et al 1994

Appendix B

Supplementary Figures for Chapter 3

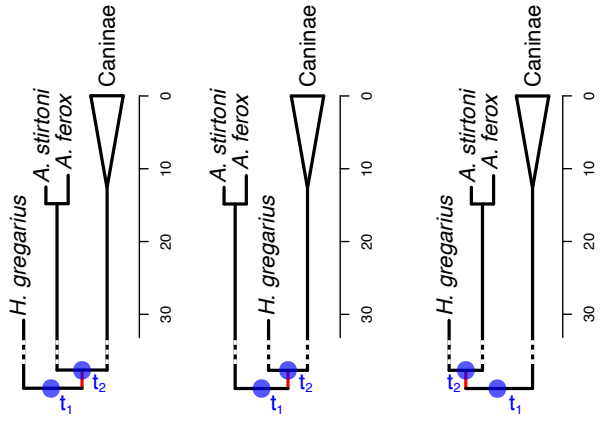

Figure B.1: The three possible ways to resolve the polytomy among the subfamilies Hesperocyoninae, Borophaginae and Caninae. Node ages for t_1 and t_2 were extracted from the posterior distribution reported by Slater (2015). Two sets of ages were used for the first and second nodes: Set I= $\{t_1 = 42.15, t_2 = 41.5\}$; and, Set II= $\{t_1 = 40.15, t_2 = 37.65\}$.

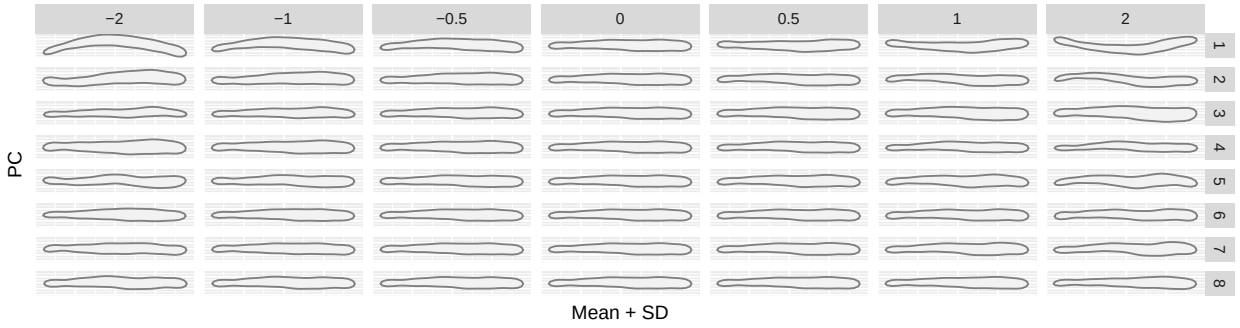

Figure B.2: Predicted outlines of bacula along different axis of the PCA analysis. The central column indicates the average morphology for all bacula included in the study. Columns to the left and right of central indicate how the average baculum changes with increments in standard deviations of the variation observed in each axis. Each row represents one PC axis.

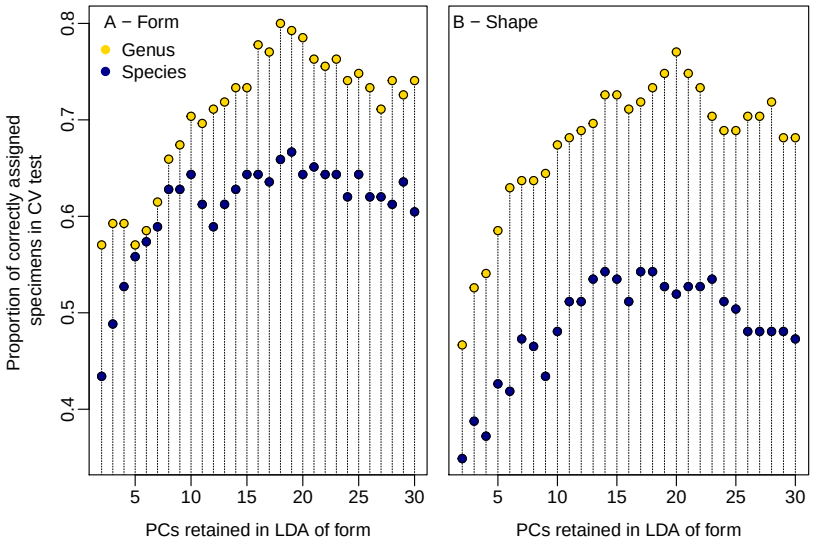

Figure B.3: Percent of specimens correctly predicted as part of their species in a leave-one-out cross-validation test of LDA depending on the number of PC retained in the analysis. A) LDA for form (size + shape). B) LDA for shape.

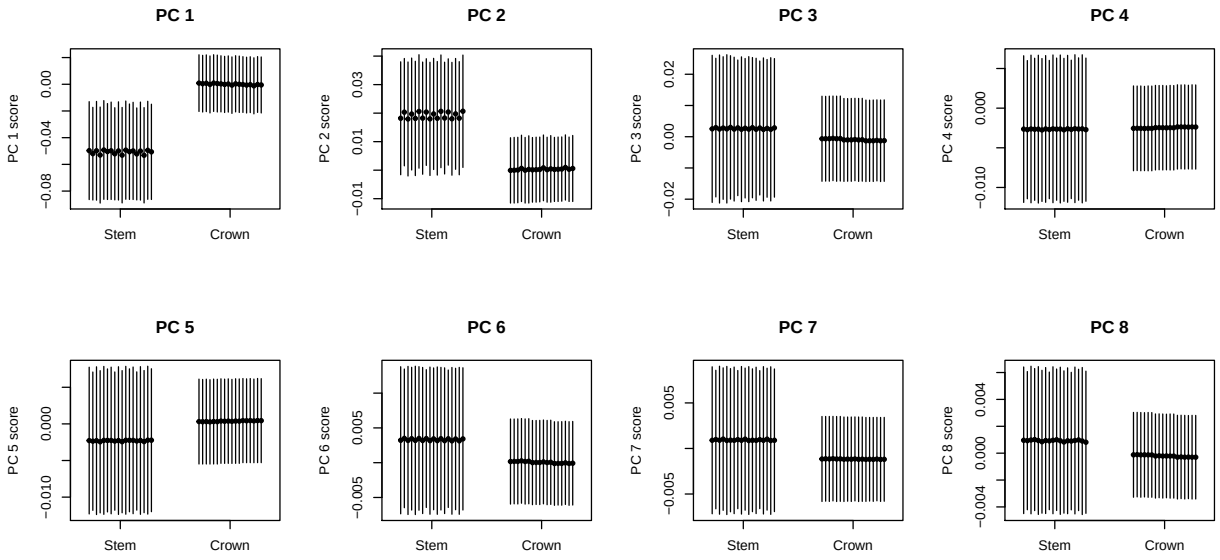

Figure B.4: Ancestral State reconstruction with its 95% confidence interval of baculum shape loadings on PC 1 to PC 8. The comparison is between the first node on the phylogeny (stem) versus the node for the crown group. This figure shows that differences for PC1 are strong regardless of the phylogenetic relationships among the three canid subfamilies. PC 2 shows slight differences between the stem and crown node reconstructions, but no differences are observed for PC3 to PC8.

Appendix C

Supplementary Figures for Chapter 4

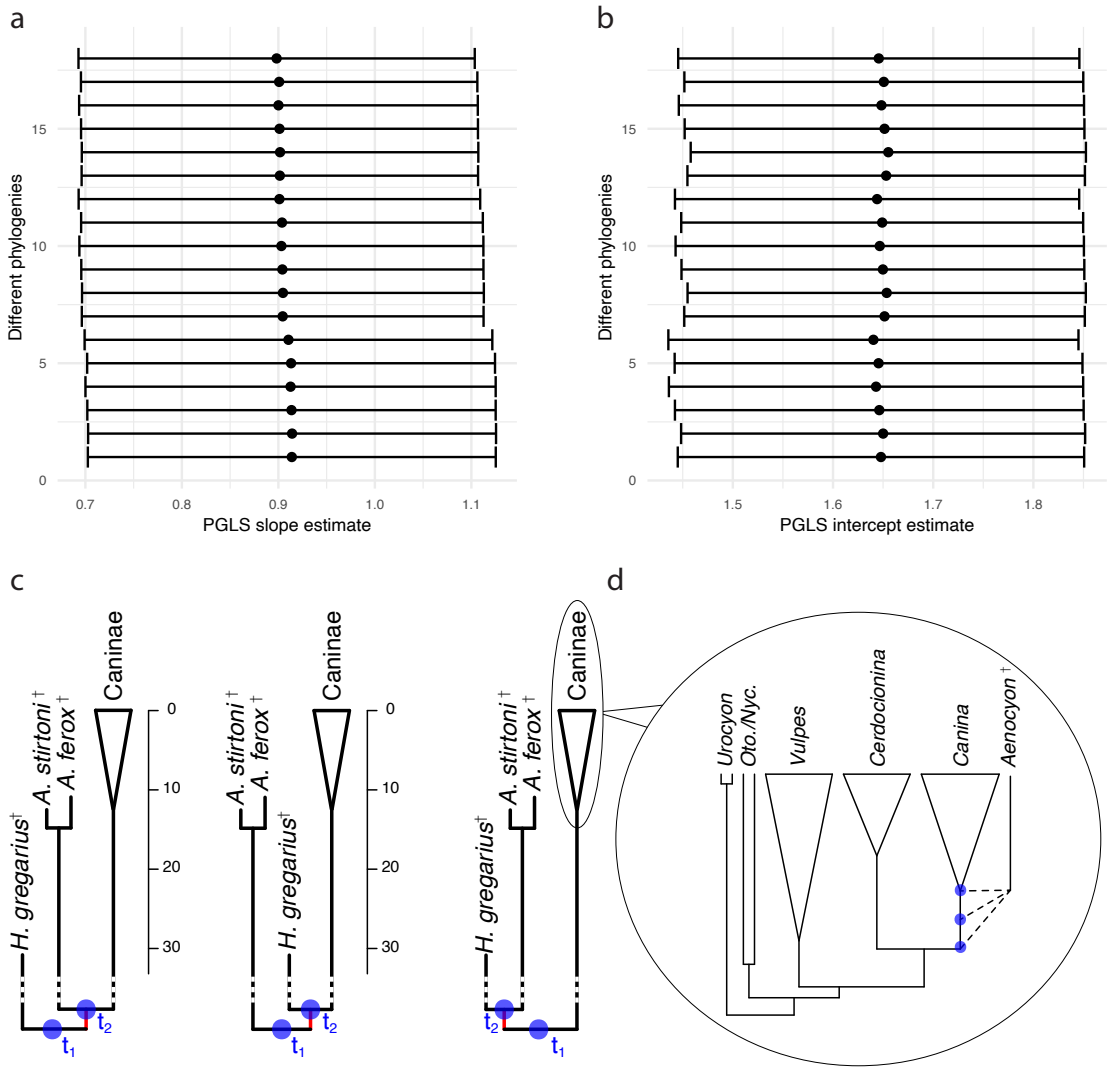

Figure C.1: Phylogenetic uncertainty in the relationship between the canines, borophagines, and hesperocyonines, and the time of divergence of the dire wolf (resulting in 18 different phylogenies) has virtually no effect on the parameter estimates from the PGLS analysis. **a:** Slope estimate. Note that isometry is within the confidence intervals in all analyses. **b:** Intercept estimate. Given the small differences among the analyses, one phylogeny was randomly chosen to show the baculum allometry in Figure 4.1a. Horizontal bars around mean estimate represent the 95% confidence intervals. **c:** The three possible ways to resolve the polytomy among the subfamilies Hesperocyoninae, Borophaginae and Caninae found by Slater (2015). Two sets of ages were used for the first and second nodes: Set $I = \{t_1 = 42.15, t_2 = 41.5\}$; and, Set $II = \{t_1 = 40.15, t_2 = 37.65\}$. **d:** Topology for Caninae from on Machado (2020) with the dire wolf (Aenocyon dirus) inserted in three positions along the stem branch of Canina, *per* relationship recovered by (Perri *et al.*, 2021)